Westerduinweg 3
1755 LE Petten
P.O. Box 15
1755 ZG Petten
The Netherlands

www.tno.nl

T +31 88 866 50 65

TNO report 2019 R10062

DOWA validation against offshore mast and LiDAR measurements

Date	21 May 2019
Author(s)	J. B. Duncan, I. L. Wijnant**, and S. Knoop**
Copy no	
No. of copies	
Number of pages	67 (incl. appendices)
Number of appendices	3
Sponsor	Supported with Topsector Energy Subsidy from the Ministry of Economic Affairs and Climate Policy
Contributing Project Parner	Koninklijk Nederlands Meteorologisch Instituut (KNMI)**
Project name	Dutch Offshore Wind Atlas (DOWA)
Project number	060.33810

Summary

The creation of the Dutch Offshore Wind Atlas (DOWA) is part of a joint project with ECN part of TNO, Whiffle, and KNMI. The DOWA is a wind atlas based on a 10-year reanalysis, which is an hourly description of the state of the atmosphere using measurements and atmospheric (weather) models. The DOWA aims to provide the developers of offshore wind power in the Netherlands with knowledge on wind conditions that is an improvement of the KNW-atlas. In order to improve upon the KNW-atlas, the DOWA uses an updated version of the global ECMWF reanalysis (ERA5), as well as an updated version of the HARMONIE numerical weather model (Cycle 40h1.2.tg2) that was used to transform the global reanalysis into a regional wind atlas. The method that was used to make the atlas was changed. The 'cold starts' within the global reanalysis used in KNW were removed and at three-hour intervals aircraft and satellite measurements were assimilated. Within this validation report, the DOWA and the KNW-atlas are validated against wind speed and direction measurements obtained from LiDARs at offshore platforms and meteorological masts.

The DOWA was developed to improve hourly correlation and to better resolve the vertical profile of wind speed without incorporating a uniform shear-correction factor. Comparison to LiDAR measurements at eight sites and to instrumented meteorological mast measurements at two locations demonstrates that the hourly correlation in the DOWA is better than in the KNW-atlas. In concrete numbers, considering all LiDAR measurement locations and heights, the mean linear regression slope increased from 0.94 (KNW) to 0.97 (DOWA) and the mean R^2 value increased from 0.87 (KNW) to 0.91 (DOWA).

Related to the above, the diurnal cycle is better represented. This, without losing significant ability to denote monthly mean and annual average wind speeds. Also, the DOWA performs similar to the KNW-atlas in its depiction of vertical changes in wind speed with height (i.e. vertical wind shear). A better representation of the diurnal cycle is demonstrated from the fact that considering all LiDAR measurement locations, the DOWA shows a reduction of hourly wind speed bias from a mean value of 1.53m/s within the KNW-atlas to a mean value of 1.27m/s within the DOWA. Also, the scatter around the mean wind speed bias is reduced; on average, the σ value of the hourly wind speed bias was reduced by 0.26m/s (16.99%).

Contents

1 Introduction

The Dutch Part of the North Sea is expected to see significant growth in wind energy production over the next decade. By 2023, the Dutch Part of the North Sea should have a total installed capacity of 4.5GW and by 2030 an installed capacity of 11.5GW. Efficient development of offshore wind requires a thorough understanding of the offshore wind conditions. While offshore wind measurements exist, they are limited both in space and time. However, by using mesoscale atmospheric models to increase the spatial and temporal resolution of global reanalyses, wind atlases can be developed to derive the offshore wind climatology at various locations and heights.

ECN published its first Offshore Wind Atlas (OWA1) in 2004 (Brand et al. 2004), which is a numerical wind atlas based on data from the Koninklijk Nederlands Meteorologisch Instituut (KNMI) HiRLAM (High Resolution Limited-area Atmospheric Model). In vertical direction the lower levels of the model were employed, i.e. in the atlas four fixed heights were considered (60m, 90m, 120m and 150m amsl; almost the same as LAT in the part of the North Sea that was considered.). OWA1 is based on the numerical data of the years 2000-2003, and was validated using data of offshore and coastal wind stations measured in the same period. A second version OWA2 (Donkers et al. 2011), an update of OWA1, was issued in 2011. Again it was based on atmospheric data from the HiRLAM, but now a longer period was considered. In addition sea depths originating from the Hydrographic Service of the Royal Netherlands Navy were used in order to estimate the wave height (sea surface roughness). The lowest levels in the vertical were used, but now three fixed heights were considered (40m, 90m and 140m amsl).

Within the past decade, KNMI has produced the KNMI North Sea Wind (KNW) atlas and within the framework of a joint project with ECN part of TNO, Whiffle and KNMI the Dutch Offshore Wind Atlas (DOWA) was developed to depict offshore wind conditions across the North Sea. The KNW-atlas is based on the global reanalysis ERA-Interim (and all measurements assimilated in this reanalysis) and was downscaled using the atmospheric model HARMONIE. A uniform (i.e. the same for all locations and all heights) wind shear correction was applied based on comparison with measurements at Cabauw. This shear-corrected KNW-atlas was validated against mast (Stepek et al. 2015) and scatterometer (Wijnant et al. 2015) wind measurements. Results demonstrated the ability of the KNW-atlas to accurately depict the long-term averaged wind speeds. Because of the method that was used to make the KNW-atlas (i.e. six-hourly ‘cold starts’ with the much coarser global reanalysis model ERA-Interim), the KNW-atlas did not exhibit a strong correlation with the hourly wind measurements. New models and methods were therefore used to make the DOWA in order to improve the hourly correlation (diurnal cycle) compared to the KNW-atlas. This report will mainly focus on examining how well the DOWA represents wind speed and direction measurements from offshore LiDARs and meteorological masts. Emphasis will be placed on how the DOWA improves hourly correlation and the representation of vertical wind shear.

This report is structured as follows: section two provides details of the measurements and models used, section three examines the performance of the wind atlas wind speeds against measurements, section four examines the performance of the wind

atlas wind directions against measurements, and section five provides a brief conclusion along with a summary of the results.

2 Atmospheric models and measurements

2.1 Reanalysis and wind atlas information

Both the KNW-atlas and the DOWA are based on a global ECMWF reanalysis and are downscaled using the atmospheric weather model HARMONIE. The two atlases employ different methods (e.g. cold start versus no cold start) and use different versions of ECMWF reanalysis and the HARMONIE weather model. Information on the models and atlases are provided below.

2.1.1 Reanalysis

Making a reanalysis involves fitting a state-of-the-art atmospheric model to historical weather measurements to obtain a spatially and temporally consistent long-term dataset that depicts the time-varying state of the atmosphere. The global ERA-Interim reanalysis was used to produce the KNW-atlas and the global ERA5 reanalysis was used to produce the DOWA. Both of these reanalysis datasets were produced by the European Center for Medium-range Weather Forecasts (ECMWF; www.ecmwf.int). More information on ERA-Interim and ERA5 is provided below.

2.1.1.1 ERA-Interim

The ERA-Interim reanalysis that was used to make the KNW-atlas combines one of the leading numerical weather prediction models (ECMWF model) with an advanced data-assimilation system (Baas 2014). The resulting analysis is considered a statistical 'best-estimate' of the state of the atmosphere at the model scales since it is based on very short-term model forecasts that have been adjusted to match observations. ERA-Interim starts in 1979 and provides three-dimensional analysis of the global atmosphere at a T255 spectral truncation (i.e. corresponding to a grid size of about 80km). The archived reanalysis dataset provides six-hourly temporal output.

2.1.1.2 ERA5

ERA5 is the fifth generation of ECMWF atmospheric reanalysis of the global climate. ERA5 will (once completely available) eventually replace ERA-Interim. The main differences between ERA-Interim and ERA5 are:

- ERA5 will eventually be available from 1950 to now (ERA-Interim 1979 to now).
- ERA5 will provide hourly data as opposed to the six-hour data produced by ERA-Interim.
- ERA5 exhibits a horizontal grid spacing of 31 km (improved relative to the ERA-Interim 80-km horizontal resolution).
- ERA5 depicts atmospheric troposphere and lower stratosphere conditions at 137 vertical levels up to about 80 km (ERA-Interim only provides 60 levels).
- ERA5 employs an updated model version of the ECMWF model (see https://confluence.ecmwf.int//pages/viewpage.action?pageId=74764925).

2.1.2 Numerical weather prediction model: HARMONIE

HARMONIE (HIRLAM ALADIN Research on Mesoscale Operational NWP In Euromed), also known by the name AROME, is the numerical weather prediction model used operationally by KNMI since 2012. It is continually being improved and tested by the HIRLAM-ALADIN consortium (Figure 1). HARMONIE is a non-hydrostatic limited-area model that runs on a high-resolution grid spacing of 2.5 km. More details regarding HARMONIE /AROME can be found in Seity et al. (2011) and online (www.hirlam.org). HARMONIE model set-up can be found in Toros et al. (2014). HARMONIE version CY37h1.1 was used to produce the KNW-atlas and HARMONIE version CY40h1.2.tg2 was used to make the DOWA. Compared to CY37h1.1, CY40h1.2.tg2 incorporates an improved turbulence parameterization (HARATU) that enables enhanced estimates of wind speed (De Rooy 2017).

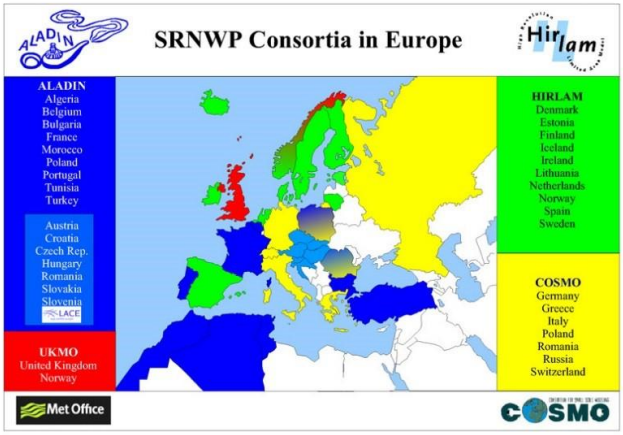

Figure 1 Participating countries in the HIRLAM (green) and ALADIN (blue) consortiums (source: http://www.eumetnet.eu).

2.1.3 Wind atlases

2.1.3.1 KNW-atlas

The KNMI[1] KNW-atlas was the first atlas based on a period long enough to capture variability in the Dutch wind climate. The KNW-atlas released in 2013 captured 40 years of atmospheric variability from 1979 to 2013. As part of the DOWA project, the KNW-atlas was extended using the same model-setup to guarantee a homogeneous dataset. The KNW-atlas will eventually encompass more than 40 years (i.e. 1979 – at least March 2019). The downscaling of ERA-Interim using HARMONIE CY37h1.1 resulted in hourly outputted data at a horizontal grid spacing of 2.5km. Wind speeds were subject to a shear-correction factor that was tuned to match wind measurements made at the 200m Cabauw tower; the shear-correction factor was uniformly applied (i.e. the same for all heights and locations) throughout the KNW domain. Prior validation of the KNW-atlas demonstrates a climatological (long-term average and once in 10-year extreme wind speeds) accuracy that (for wind turbine hub heights typical of the period [~80m]) is comparable to that of measurements. The accuracy of the long-term average wind speeds is less than 0.2m/s at higher heights. Additional

[1] The KNW-atlas is financed by the Directorate-General for Spatial Development and Water Affairs (DGRW) of the Dutch Ministry of Infrastructure and the Environment (IenM), now called the Ministry of Infrastructure and Water Management (IenW): https://www.government.nl/ministries/ministry-of-infrastructure-and-water-management

information on the KNW-atlas can be found online (http://projects.knmi.nl/knw/index.html).

2.1.3.2 DOWA

Creating the DOWA[2] was part of a joint project with ECN part of TNO, Whiffle, and KNMI. The DOWA is a wind atlas based on a 10-year (2008-2017) reanalysis and is expected to improve hourly wind correlation. It comprises a better physical representation and a better time resolution which are important in wind energy applications and which are expected to improve the knowledge on the wind in the covered area. On the other hand, due to the limited time span of the DOWA, it cannot adequately capture North Sea wind climate variability like the KNW-atlas. Therefore, the DOWA is not expected to provide any significant improvements to the climatological accuracy of the KNW-atlas. Furthermore, the DOWA atlas provides wind information up to 600m heights and includes information that can enable Large Eddy Simulation (LES) downscaling from hourly data to less than 60s and from a 2.5km horizontal resolution to less than 100m horizontally. The DOWA domain is also larger than that of the KNW-atlas (Figure 2). It is defined by a 789 by 789 grid centered around the KNMI meteorological mast Cabauw that is a part of the Cesar observatory[3].

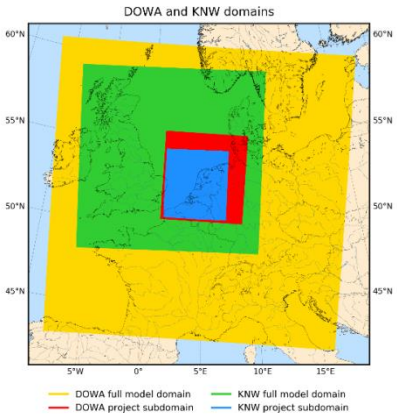

Figure 2 The DOWA was made and saved on a domain of 789 by 789 points centered around Cabauw (yellow area). The shaded portions depict the DOWA and the KNW-atlas domains.

In addition to using new models (i.e. ERA5 instead of ERA-Interim and HARMONIE CY40h1.2.tg2 instead of CY37h1.1), new methodologies were implemented within the DOWA, which are detailed in the bullets below.

- **Assimilation of measurements:**
    - For the KNW-atlas, no additional measurements were assimilated into HARMONIE during the process of downscaling (i.e. the only measurements used were the ones assimilated in the ERA-Interim reanalysis).

[2] The DOWA-project is financed by the Ministry of Economic Affairs and Climate Policy (SDE+ Hernieuwbare Energie Call)

[3] https://www.knmi.nl/kennis-en-datacentrum/uitleg/meetmast-cabauw ; http://www.cesar-observatory.nl/index.php?pageID=7001

- For the DOWA, the full potential of HARMONIE as a weather forecasting model was leveraged by assimilating additional measurements (both conventional and innovative) that were not used in ERA5. Innovative measurements included high-resolution satellite surface wind fields (Advanced Scatterometer [ASCAT]) and aircraft wind profile measurements (MODE-S EHS). The 3DVAR assimilation technique was used to assimilate these measurements at three-hour intervals at the beginning of each HARMONIE forecast cycle (see 'cold start' discussion below). Using these additional measurements is expected to improve the quality of the time series and provide a more detailed depiction of the diurnal cycle.

- **Cold start:**

  - For the KNW-atlas, each six-hour forecast period started with the ERA-Interim reanalysis (cold start). Subsequently, HARMONIE (using no additional data assimilation) was used to produce the +1 hr up to the +6 hr forecast.

  - Except at the beginning of each parallel stream[4], no cold starts were used in the DOWA. The DOWA is comprised +1 hr, +2 hr, and +3 hr HARMONIE forecasts. At each hour, the boundaries of the DOWA domain (North, South, East, and West at all model levels) are fed with ERA5 reanalysis data, and each three-hour forecast cycle is initialized using the latest HARMONIE forecast of the previous cycle (i.e. no cold starts with ERA5 data) and data-assimilated measurements.

Relevant differences between the KNW-atlas and the DOWA are summarized in Table 1. Additional DOWA details can be found online (http://www.dutchoffshorewindatlas.nl/).

Table 1 Relevant differences between the KNW-atlas and the DOWA.

KNMI North Sea Wind (KNW) Atlas	Dutch Offshore Wind Atlas (DOWA)
1979 – 2019 (40 years)	2008 – 2017 (10 years)
Captures the variability of the North Sea wind climate	Does not capture the variability of the North Sea wind climate
Based on ERA-Interim reanalysis and the mesoscale weather model HARMONIE Cycle 37h1.1	Based on ERA5 reanalysis (follow-up of ERA-Interim with higher spatial and temporal resolution) and the mesoscale weather model HARMONIE Cycle 40h1.2.tg2 (improved wind information because turbulence is modelled better)
HARMONIE only used as downscaling tool (data assimilation of measurements in ERA-Interim only)	Additional HARMONIE data assimilation (ASCAT-satellite surface wind measurements and MODE-S-EHS aircraft wind profile measurements)
Climatological information up to and including a height of to 200 m	Climatological information up to and including a height of 600 m
Lacks the information required for further LES-downscaling	Includes the information required for further LES-downscaling
Cold starts: limited quality of hourly correlation with measurements (e.g. diurnal cycle)	No cold starts: better hourly correlation with measurements and representation of the diurnal cycle
Uniform wind shear correction applied	No wind shear correction required

[4] Stream A (2010-2012), stream B (2013-2014), stream C (2008-2009) and stream D (2015-2017) were run simultaneously to speed up calculations (it takes about 1 month to calculate 4 months) and then glued.

2.2 Validation measurement information

Wind data measured by LiDAR (both platform-mounted and floating) and instrumented meteorological masts (cup anemometers and wind vanes) were used in this study to examine the performance of the two wind atlases (KNW-atlas and DOWA). Measurements at nine different sites were used for validation (Figure 3). Measurements were made within the Borssele Wind Farm Farm Sites I (BWFZ1) and II (BWFZ2), the Hollandse Kust Noord (HKN) and Zuid (HKZ) wind farm zones, the Offshore Windpark Egmond aan Zee (OWEZ), and at several other offshore platforms including the Europlatform (EPL), K13a, IJmuiden (MMIJ), and Lichteiland Goeree (LEG). At measurement sites HKN and HKZ, two LiDARs were deployed within the wind farm zone. Data from these floating LiDARs were analysed separately and are differentiated with the suffixes a and b (i.e. HKNa and HKNb) in the presented results. LiDAR and mast measurement specifics are provided in the following subsections and data quality control procedures are documented in Appendix A.

Information on the specific offshore measurement platforms and their installation details can be found online at www.windopzee.net and in Section 2.2 of the ECN part of TNO report titled 'Understanding of the Offshore Wind Resource up to High Altitudes (≤315 m)' (Duncan et al. 2018). The latter report also contains information on data availability.

The meteorological masts are IEC compliant (IEC 2005) and their wind instrumentation is calibrated according to MEASNET procedures. All fixed LiDARs were verified prior to their specific installation offshore, for which references are provided in the section below. It is made sure that the type of floating LiDAR system used, is commercial mature according to the OWA roadmap (Carbon Trust 2013) and the recommended practices for the use of floating LiDAR systems (Bischoff et al. 2016). Furthermore and according to the same procedures, all individual systems are validated before their specific use offshore. Information on these individual validations is provided on the RVO website (https://offshorewind.rvo.nl).

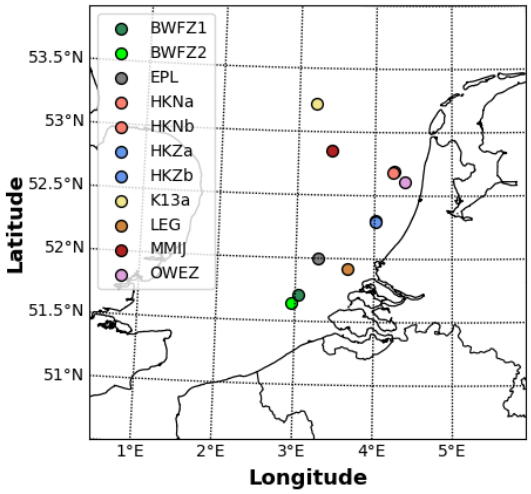

Figure 3 Location of the nine measurement sites used for validation of the two wind atlases. LiDAR measurement location within HKN (i.e. HKNa and HKNb) and HKZ (i.e. HKZa and HKZb) are not significant enough to appear within the spatial map and therefore are plotted with the same measurement colour.

2.2.1 LiDAR measurements

Vertically pointing LiDAR provides efficient and non-intrusive measurement of atmospheric winds. Compared to traditional meteorological masts, LiDAR typically expands the maximum measurement height and the total number of measurement levels. LiDAR(s) were deployed at eight of the nine measurement sites; however, LiDAR type and mounting procedures varied between sites. LiDAR type included the Zephir 300s continuous-wave (CW) LiDAR and the WINDCUBE v2 pulsed LiDAR. The LiDARs at MMIJ, K13a, EPL, and LEG were mounted on a fixed platform, while the LiDARs at BWFZ1, BWFZ2, HKN, and HKNZ were instrumented atop a floating metocean buoy.

CW and pulsed wind LiDAR are coherent systems that utilize the Doppler effect to extract an estimate of the radial wind speed (i.e. the component of the velocity vector that points directly towards or away from the LiDAR). Therefore, unless the wind is moving directly along the radial, the velocity vector will not be fully resolved. For wind resource assessment, it is imperative to know the horizontal velocity vector—not the radial wind speed—at multiple heights. In order to resolve the vertical profile of the horizontal velocity vector, both CW and pulsed wind LiDAR use varying adaptations of conical scanning techniques (Banakh et al. 1993). While these techniques are not discussed in detail, they allow the CW wind LiDAR to resolve the vertical profile of the horizontal wind field at 17-s intervals and enable the pulsed wind LiDAR to resolve the vertical profile of the horizontal wind field at 4-s intervals. Prior to analyses, the profile data is averaged to produce 10-min average statistics.

A summary of the LiDAR measurements at each site—including LiDAR type, mounting procedure, measurement heights, and the data collection period—is provided in Table 2. A schematic is also provided in Figures 4 and 5 to demonstrate the measurement site LiDAR sampling heights and the data collection period. While not reflected in Figures 4 and 5, the measurement heights at MMIJ, HKN, HKZ, and BWFZ are defined relative to the lowest-astronomic tide, while the measurement heights at EPL, LEG, and K13a are defined relative to the mean sea level. Slight differences between the lowest-astronomic tide and mean sea level (i.e. the lowest-astronomic tide is on average 1.06 m below the mean sea level) are not expected to significantly impact the DOWA validation. Also, not all of the LiDAR measurements could be used for the DOWA validation because measurements that were affected by the wake of neighbouring wind farms were removed (see Section 2.3). A wind direction filter was used to exclude wake-impacted wind measurements at HKN, HKZ, and BWFZ.

Table 2 Measurement site LiDAR description. Data collection period start and end times are denoted by the letters S and E and measurement heights are indicated by HGT_{min}:$HGT_{interval}$:HGT_{max} and any other measurement heights.

Measurement Location Identifier	LiDAR Type (x 2—two site LiDARs)	Mounting Procedure	Measurement Heights (m)	Data Collection Period
MMIJ	ZephIR 300s	Platform Mounted	90:25:315	S: 01-Nov-2011 E: 09-Mar-2016
EPL	ZephIR 300s	Platform Mounted	91:25:291 and 63	S: 30-May-2016 E: 31-Dec-2017
LEG	WINDCUBEv2	Platform Mounted	91:25:291 and 63	S: 17-Nov-2014 E: 31-Dec-2017
K13a	ZephIR 300s	Platform Mounted	91:25:291 and 63	S: 01-Nov-2016

HKN	ZephIR 300s x 2 (Sites A and B)	Floating	60:20:200 and 30 and 40	E: 31-Mar-2018 S: 10-Apr-2017 E: 31-Oct-2017 **Period A = Period B**
HKZ	ZephIR 300s x 2 (Sites A and B)	Floating	60:20:200 and 30 and 40	S: 05-Jun-2016 E: 28-Feb 2018 **Period A = Period B**
BWFZ	ZephIR 300s x 2 (Sites I and II)	Floating	60:20:200 and 30 and 40	**Site I:** S: 11-Jun-2015 E: 27-Feb-2017 **Site II:** S: 12-Feb-2016 E: 07-Jul-2016

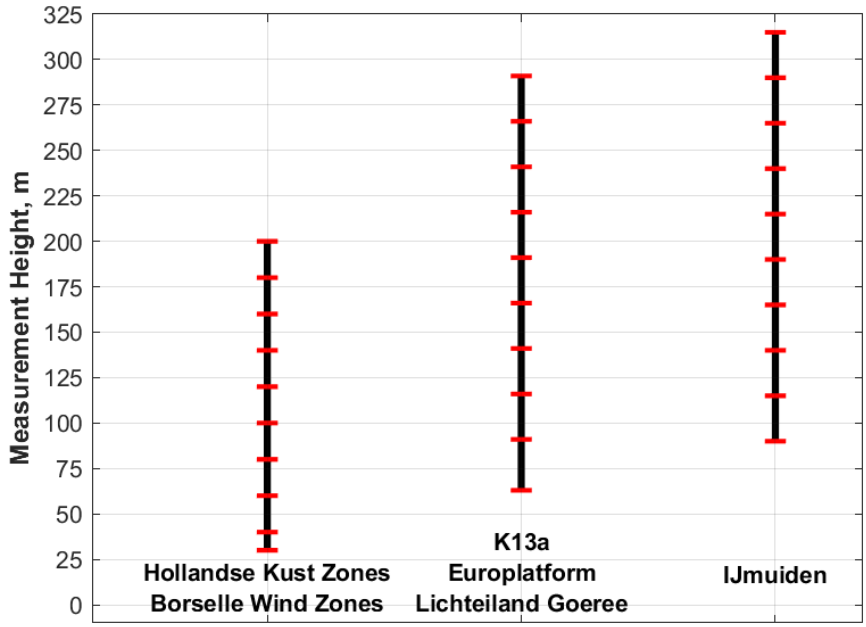

Figure 4 Measurement site LiDAR sampling heights (horizontal red lines).

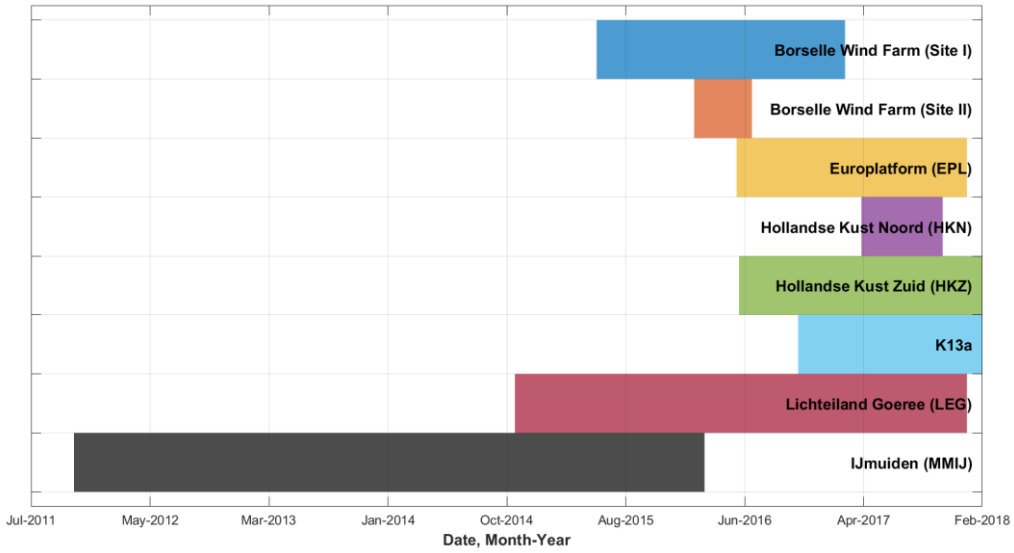

Figure 5 Measurement site data collection periods.

Uncertainty assessment

The fixed (platform mounted) LiDARs have been compared to anemometer and vane measurements on an IEC compliant meteorological mast at the Lidar Calibration Facility (ELCF) of the ECN Wind Turbine test site Wieringermeer (EWTW). These measurements are performed according IEC61400-12-1 and MEASNET procedures for power performance measurements and are of the highest possible quality[5] and have a wind speed uncertainty of less than 0.2 m/s for the wind energy relevant wind speed region (1.8%-1.2% in the wind speed range 4m/s-16m/s). For details on these mast uncertainties reference is made to the individual LiDAR verification reports. From the various verifications the following details are extracted:

- The ZephIR 300 (unit 315) that is mounted on the EPL platform was compared to an IEC compliant meteorological mast at the ECN part of TNO's LiDAR Calibration Facility from 24-04-2018 until 07-06-2018. The results are described in Wouters et al. (2019) and exhibit an uncertainty at 90m ranging from 1.9%-2.7% in the wind speed range 4m/s-16m/s, excluding sensitivity.
- The ZephIR 300M (unit 563) that is mounted on the K13a platform was compared to an IEC compliant meteorological mast at the ECN part of TNO's LiDAR Calibration Facility from 31-8-2016 until 10-10-2016. The results are described in Wouters et al. (2019) and exhibit an uncertainty at 90m ranging from 1.7%-2.3% in the wind speed range 4m/s-16m/s, excluding sensitivity.
- The Leosphere Windcube (WLS7-577) that is mounted on the Lichteiland Goeree platform was compared to an IEC compliant meteorological mast at the ECN part of TNO's LiDAR Calibration Facility from 17-11-2016 until 14-04-2017. The results are described in Wouters et al (2019) and exhibit an uncertainty at 90m ranging from 2.1%-2.9% in the wind speed range 4m/s-16m/s, excluding sensitivity.
- The ZephIR 300 that is mounted on the MMIJ platform was compared to the IEC compliant meteorological mast Ijmuiden itself. Among others an uncertainty assessment of the LiDAR is described in Maureira Poveda et al. (2015) and reports an uncertainty at 90m ranging from 1.2%-2.2% in the wind speed range 4m/s-16m/s, excluding sensitivity.

The above verification tests have been performed at specific locations and so the results may be subject to local conditions. To use the uncertainty results also for other locations, f.i. on the offshore platforms, an uncertainty contribution due to the sensitivity to local conditions needs to be added conform IEC 61400-12-1 Annex L. Because the in this standard described procedure is not without ambiguity at least the LiDAR uncertainty without the sensitivity contribution has been reported above. For the Windcube V2, Albers et al. (2013), report a sensitivity contribution of 1.5%. For the Zephir 300 we could only find a report of the LiDAR manufacturer itself (Medley 2014) reporting a sensitivity contribution of 1.7%-2.2%. Adopting a conservative approach, the 2.2% contribution is used in this work.

[5] At MMIJ first class advanced cup anemometers (Werkhoven et al. 2012) are used

Table 3: Overview of LiDAR platforms and their verification uncertainty, sensitivity uncertainty and total uncertainty during on site measurements

Platform	Verification uncertainty	Sensitivity uncertainty	Total uncertainty
EPL	1.9%-2.7%	2.2%	2.9%-3.5%
K13a	1.7%-2.3%	2.2%	2.7%-3.2%
LEG	2.1%-2.9%	1.5%	2.6%-3.3%
MMIJ	1.2%-2.2%	2.2%	2.5%-3.1%

For the floating LiDARs used at HKN, HKZ and BWFZ and here used for the validation of the DOWA, the uncertainty assessment is based on the type verification test performed at the IEC compliant meteorological mast IJmuiden comprising cup anemometer and vane measurements (Stein et al. 2015; Wagenaar et al. 2015). The instruments in this mast are calibrated according MEASNET procedures. A floating LiDAR uncertainty assessment for this system is provided in Dhirendra et al. (2016) (approved by ECN) and exhibit an uncertainty at 92m ranging from 2.0%-3.4% in the wind speed range 4m/s-16m/s, excluding sensitivity.

A first attempt to quantify the floating LiDAR uncertainty contribution due to sensitivity was made in Wagenaar et al (2015) leading to rather large total uncertainty range at 92m of 2.97%-6.22% in the wind speed range 4m/s-16m/s. In Dhirendra et al. (2016) a modest sensitivity uncertainty contribution was adopted leading to a total uncertainty range at 92m of 3.1%-4.2% in the wind speed range 4m/s-16m/s.

2.2.2 Instrumented meteorological masts

A meteorological mast instrumented at multiple levels was located at both MMIJ and OWEZ. The MMIJ meteorological mast was instrumented with cup anemometers at 27m, 58m, and 92m and with a sonic anemometer at 85m to measure horizontal wind speed, and was equipped with wind vanes at 27m, 58m, and 87m to measure horizontal wind direction. The OWEZ meteorological mast was instrumented with cup anemometers and wind vanes at 21m, 70m, and 116m to measure horizontal wind speed and direction. At each measurement height and location, the anemometry (cup anemometers and wind vanes) was mounted along three boom arms. Anemometry at MMIJ was mounted to booms arms at 46.5º (~NE), 166.5º (~SSE), and 286.5º (~WNW), while anemometry at OWEZ was mounted to boom arms at 60º (~NE), 180º (S), and 300º (~NW). Measurements were made along multiple boom arms in order to make measurement of the undisturbed wind possible. Depending upon the wind direction, wind measurements from different boom arms were used to mitigate the impact of the tower structure on the wind (see Appendix A).

A summary of the meteorological mast measurements at MMIJ and OWEZ—including anemometer type (i.e. cup and vane), measurement heights, and the data collection period—is provided in Table 4. A schematic is also provided in Figure 6 and 7 to demonstrate the mast measurement heights and the data collection period. A wind direction filter was used to exclude wake-impacted wind measurements at OWEZ.

Table 4 Measurement site mast description. Data collection period start and end times are denoted by the letters S and E.

Measurement Location Identifier	Anemometry Type	Measurement Heights (m)	Data Collection Period
MMIJ	This First Class Advanced Cup Anemometer, METEK USA-1 sonic anemometer and Wind Vane	WS: 27, 58, 85, 92 WD: 27, 58, 87	S: 02-Nov-2011 E: 11-Mar-2016
OWEZ	Mierij Meteo Cup Anemometer and Wind Vane	21, 70, 116 $WS_{HGT} = WD_{HGT}$	S: 01-July-2005 E: 31-Dec-2010

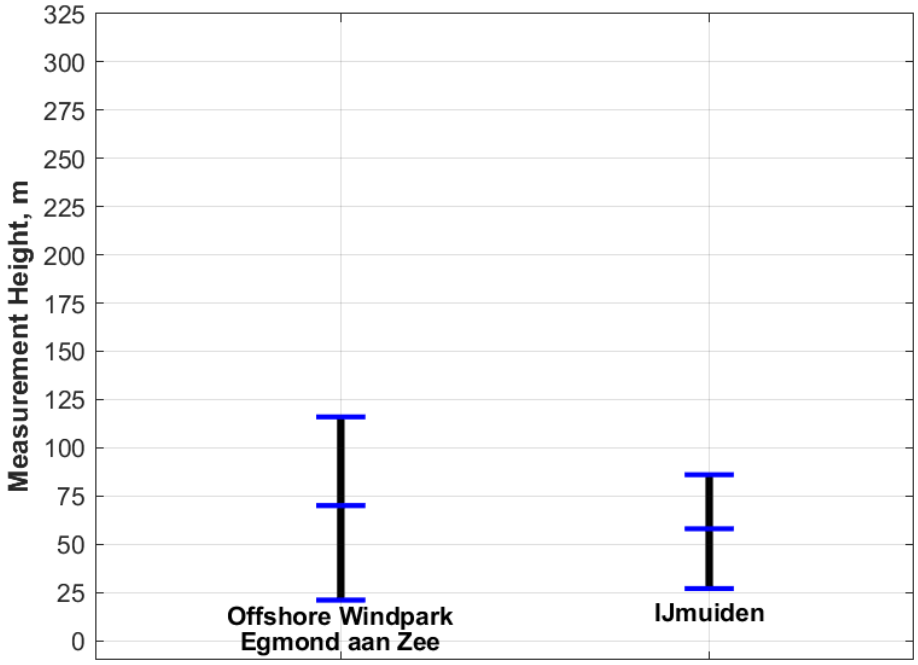

Figure 6 Measurement site mast sampling heights (horizontal blue lines).

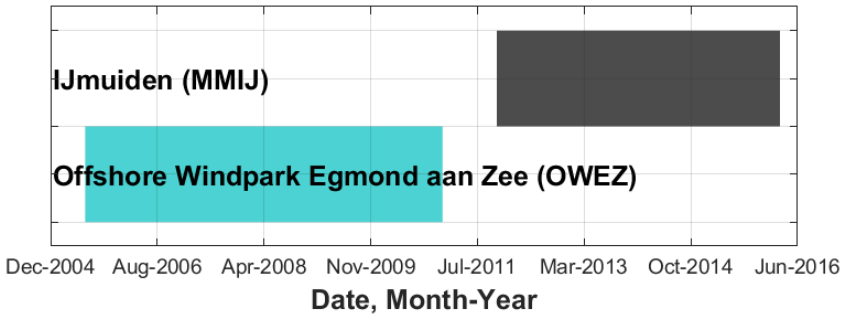

Figure 7 Measurement site data collection periods.

Uncertainty assessment

As argued the meteorological mast IJmuiden layout and its specific instrumentation is according to IEC 61400-12-1 standard and MEASNET procedures. The uncertainty analysis presented here results from the same standard and details the following uncertainty components: uncertainty due to calibration, operational characteristics, mounting and data acquisition. The details of the specific instrumentation is provided in Werkhoven (2012).

- Calibration: The cup anemometer is calibrated in the wind tunnel for which we estimate the uncertainty to be 0.031m/s (see for instance Wouters et al,

2019). The sonic anemometer specifications (METEK 2013) state a resolution of 0.1m/s.

- Operational characteristics. The cup anemometer is of class 0.9A (https://www.nrgsystems.com/products/met-sensors/anemometers/detail/thies-first-class-advanced-anemometer) and we estimate the sonic anemometer to be of class 5.3A based on a comparable system (Westermann 2019). According to IEC 61400-12-1 the associated uncertainties are

$$u_{v,op,cup} = (0.5\% + 0.05\mathrm{m/s}) * \frac{0.9}{\sqrt{3}}$$
$$u_{v,op,sonic} = (0.5\% + 0.05\mathrm{m/s}) * \frac{5.3}{\sqrt{3}}$$

- Mounting. There are 2 side mounted cup anemometers at the top (92m), 3 boom mounted sonic anemometers at 85m and 3 boom mounted cup anemometers at the remaining levels of 58m and 27m. We estimate the uncertainty due to mounting of the
  - side mounted cup anemometers at the top to be 1%,
  - boom mounted sonic anemometers to be 1.5%,
  - boom mounted cup anemometers to be 1.5%
- Data acquisition. The data of the cup anemometers are acquired using a Dante Frontend. The sonic anemometer provides a digital output, so there is no uncertainty component. We estimate the associated uncertainties to be

$$u_{v,dacq,cup} = 0.43\% + 0.017\mathrm{m/s}$$
$$u_{v,dacq,sonic} = 0\mathrm{m/s}$$

Quadratically adding all contributions we estimate the uncertainty in the wind speed measurements at the various heights at MMIJ to be

- 92m: 1.8%-1.2% in the wind speed range 4m/s-16m/s
- 85m: 4.8%-1.9% in the wind speed range 4m/s-16m/s
- 58m/27m: 2.1%-1.7% in the wind speed range 4m/s-16m/s

For the wind speed measurements at the OWEZ meteorological mast various background information exist (Eecen 2007; Crockford 2015; Kouwenhoven 2017; www.noordzeewind.nl) and based on this we adopt a wind speed uncertainty of 3.4% (see particularly Crockford 2015).

2.3 Development of comparable collocated datasets

Fundamental differences exist (temporal and spatial) between the wind atlas data and measurements. The wind atlas data (the KNW-atlas and the DOWA) is provided at one-hour intervals (i.e. 00:00 UTC, 01:00 UTC, etc.) and it represent a best estimate of the wind conditions at that hour for a 2.5km by 2.5km grid box. Wind atlas data are therefore instantaneous volume averages, whereas the measurement data (LiDAR and mast) are 10-min temporal averages at the measurement location. In the mast/LiDAR validation report of the KNW-atlas (Stepek et al. 2015), it was argued that the instantaneous volume-averaged KNW-atlas values should be each compared to an hourly averaged measurement value. Therefore, measurements from a half-hour before and a half-hour after the wind atlas hour (i.e. six total 10-min mean measurements) were averaged (scaler averages as opposed to vector averages) to produce an hourly measurement value that could be used for validation.

Because the measurement time stamp refers to the beginning of the 10-min averaging period, measurements at 00:30 UTC (i.e. referring to the time period between 00:30 UTC and 00:40 UTC), 00:40 UTC, 00:50 UTC, 01:00 UTC, 01:10 UTC, and 01:20 UTC were averaged to validate the wind atlas wind speed and direction values at 01:00 UTC. An analogous 'one-hour' measurement value was derived as long as there was at least one valid measurement (i.e. the measurement passed the quality control measures described in Appendix B) within the one-hour period.

Adjustments were also made to account for height differences between the wind atlases and measurements. A cubic-spline interpolation scheme was used to interpolate the wind atlas data to the site-specific measurement heights in order to account for the height differences. Linear interpolation was also examined as a means to interpolate to the site-specific measurement heights. However, validation statistic differences as a result of the interpolation technique used were relatively insignificant. Furthermore, for validation of the wind atlas wind speeds and directions, measurement data were compared to wind data from the nearest wind atlas grid cell.

The statistics provided in Section 3 are derived from collocated datasets (i.e. a wind atlas value was only considered when an hourly measurement value was also defined). Also, only measurements (wind speed and direction) that did not have the potential to be disturbed by neighboring wind farms and their wake were used in the presented analyses. Therefore, not all of the measurements detailed in Tables 2 and 3 were used for validation. More information on the filtering that was used to remove wind farm wake effects is provided in Appendix B.3.

3 Validation of the DOWA wind speeds

Validation of the DOWA is carried out against LiDAR and instrumented meteorological tower measurements. The performance of the DOWA is examined relative to that of the KNW-atlas. Specifically, discussion is provided within the framework of the objectives of the DOWA (i.e. how does the DOWA improve the representation of the vertical wind shear and hourly correlation compared to the KNW-atlas?).

This validation report generally conforms to what was done for the validation of the KNW-atlas (Stepek et al. 2015), but an assessment of the hourly wind speed correlation between the wind atlases and measurements is also included. Whereas the KNW-atlas validation focused on 80-m heights, the DOWA validation focuses on 100-m heights. This change was instituted, in part, to the growing size of offshore wind turbines. It will be explicitly noted in text if the purported statistics do not correspond to the measurement height nearest 100 m. Bias is defined herein as the measurement minus wind atlas value (i.e. $WS_{meas} - WS_{atlas}$). Therefore, a positive bias indicates that the DOWA underestimates the wind speed while a negative bias indicates that the DOWA overestimates the wind speed. While statistics are provided for K13a, results should be interpreted with caution as analyses by Sengers (2019) indicates significant (and anomalous compared to that observed at other measurement locations) mean absolute errors in wind speed (1.80m/s).

The chapter is structured as follows: Section 3.1. examines hourly correlation at multiple heights, Section 3.2. examines the seasonal and diurnal average wind speeds, Section 3.3. examines the Weibull distribution at multiple heights, and Section 3.4 examines the monthly and annual average wind speeds. Within each section, the validation of the DOWA against LiDAR measurements is presented separately (e.g. Section 3.1.1) from that of the instrumented meteorological tower measurements (e.g. Section 3.1.2).

3.1 Hourly correlation at multiple heights

A principal focus of the DOWA was to improve the hourly correlation with measurements. Hourly correlation was examined using linear least-squares regression, which defines the linear relationship between two variables (i.e. x and y) as $y = mx + b$, where m is the slope of the line and b is its y-intercept. Within the presented analyses, the measured (i.e. LiDAR or mast) wind speed is taken to be the x-value and the wind atlas (i.e. the KNW-atlas or the DOWA) wind speed is taken to be the y-value (i.e. $WS_{Atlas} = slope * WS_{Meas} + y_{intercept}$). Given a slope value of one, which indicates that a unit change in the measured wind speed corresponds on average to a unit change in the wind atlas wind speed, the y-intercept value gives an indication of the mean bias. The value of R^2 denotes the clustering (i.e. precision) of the data about the fitted linear regression line, and the square root of R^2 (i.e. R) is the correlation coefficient. Therefore, improved performance of the DOWA compared to the KNW-atlas would be indicated by: (1) an R^2 value closer to one (i.e. $R^2 \rightarrow 1$), a (2) a slope value closer to one (i.e. $slope \rightarrow 1$), and (3) an intercept value closer to zero (i.e. $intercept \rightarrow 0$).

3.1.1 Validation of the DOWA against offshore LiDAR

The DOWA wind speeds were plotted against the LiDAR wind speeds at the measurement height nearest 100m in the left column of Figures 8 through 17 for each LiDAR measurement location. The slope, y-intercept, and coefficient of determination (R^2) of the linear least-squares regression fit at this measurement height and for these measurement locations is provided in Table 5 for the KNW-atlas and the DOWA. Further, vertical changes in the value of the linear least-squares regression slope and R^2 for both the DOWA and the KNW-atlas are provided in the right column of Figures 8 through 17 for each LiDAR measurement location. The main conclusion is that at each LiDAR measurement location and height, the values of both the linear least-squares regression slope and R^2 indicate improved hourly correlation within the DOWA. The mean slope value was 0.97 within the DOWA and 0.94 within the KNW-atlas, while the mean R^2 value was 0.91 within the DOWA and 0.87 within the KNW-atlas. The correlation statistics were fairly constant with height within the DOWA. This means that incorporating a shear-correction factor is not needed within the DOWA as it was within the KNW-atlas in order to adequately depict changes in wind speed with height. The slope, y-intercept, and R^2 value of the linear least-squares regression fit was significantly worse at BWFZ than at the other LiDAR measurement locations.

Table 5 The slope, y-intercept, and R^2 values derived from performing linear least-squares regression between the wind atlas and LiDAR wind speeds.

Measurement Location Identifier (hgt)	**Slope Value (KNW | DOWA)**		**Y-Intercept Value (KNW | DOWA)**		**R^2 Value (KNW | DOWA)**	
MMIJ (90 m)	0.97	0.98	0.30	0.20	0.91	0.93
K13a (91 m)	0.96	1.00	0.46	0.18	0.89	0.93
HKNa (100 m)	0.93	0.97	0.44	0.18	0.87	0.92
HKNb (100 m)	0.92	0.97	0.58	0.25	0.86	0.92
HKZa (100 m)	0.94	0.99	0.44	0.19	0.88	0.92
HKZb (100 m)	0.95	0.99	0.41	0.17	0.89	0.92
EPL (91 m)	0.94	0.98	0.46	0.27	0.87	0.92
LEG (91 m)	0.97	1.00	0.25	0.15	0.90	0.93
BWFZ1 (100 m)	0.89	0.93	1.00	0.64	0.83	0.88
BWFZ2 (100 m)	0.91	0.93	0.80	0.56	0.84	0.88

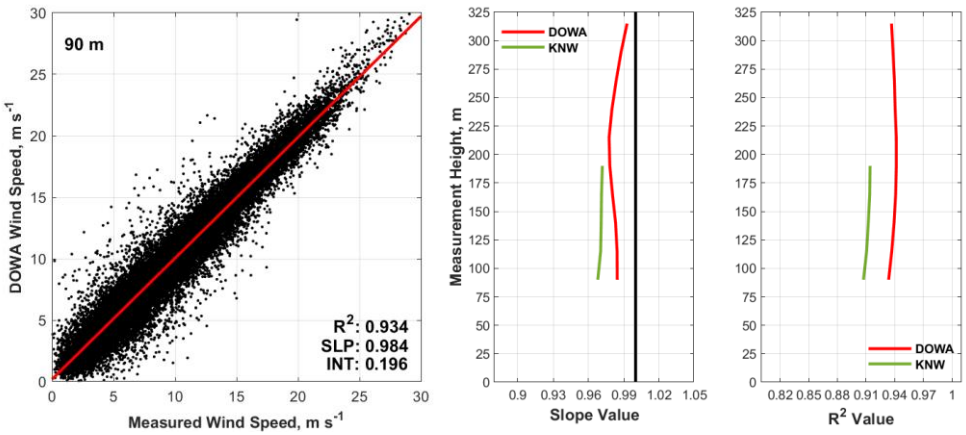

Figure 8 (Left column) Scatterplot of the DOWA and LiDAR wind speeds at MMIJ. (Right column) Vertical differences in the value of the linear least-squares regression slope and R^2.

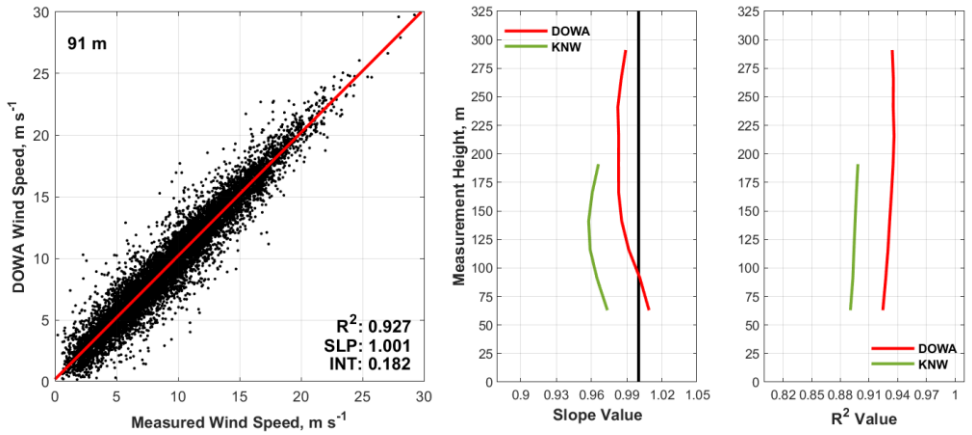

Figure 9 Same as Figure 8 except at K13a.

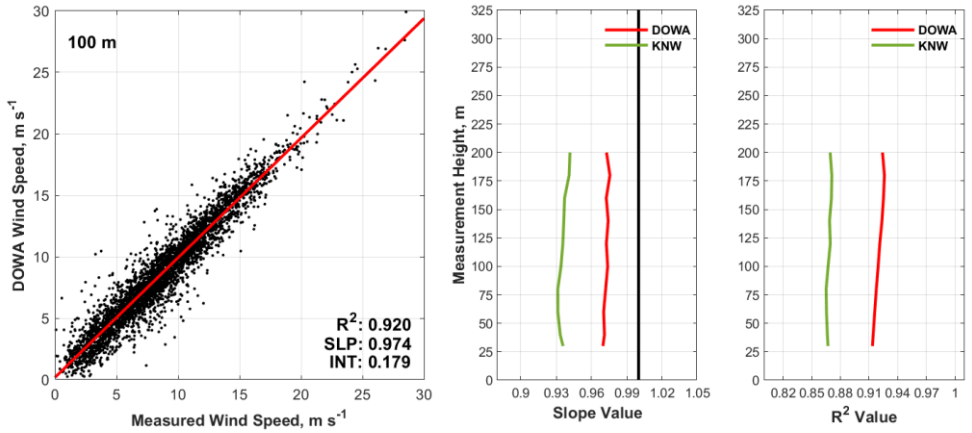

Figure 10 Same as Figure 8 except at HKNa.

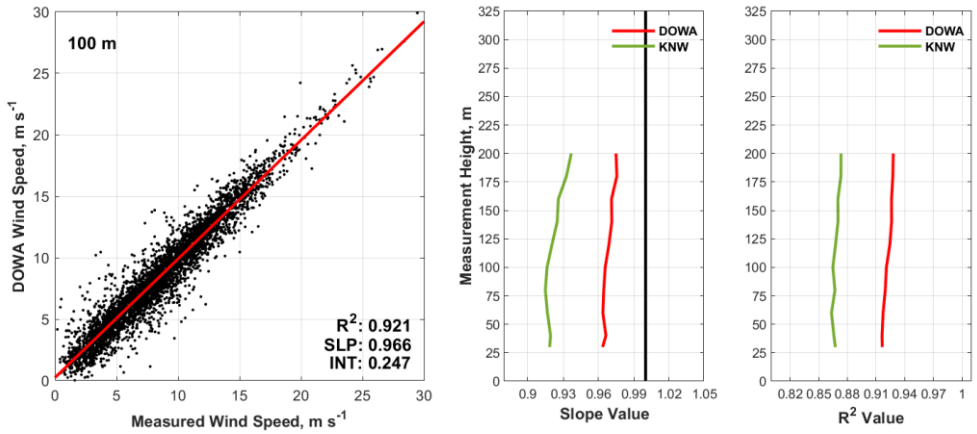

Figure 11 Same as Figure 8 except at HKNb.

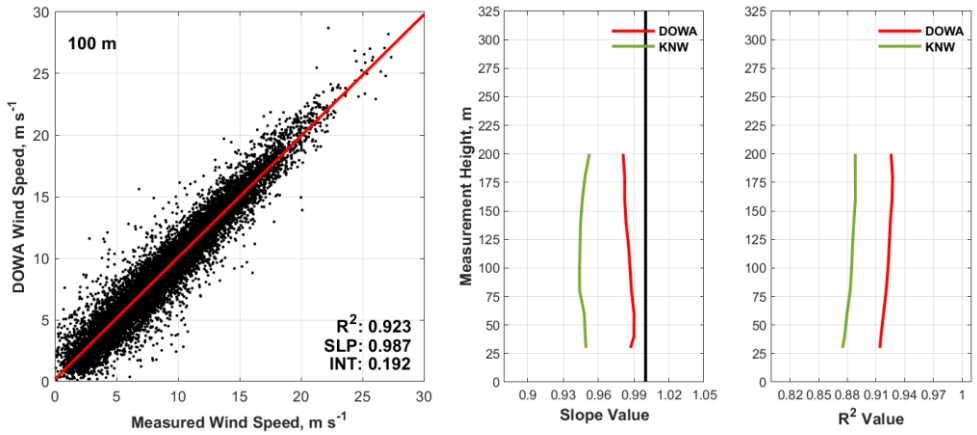

Figure 12 Same as Figure 8 except at HKZa.

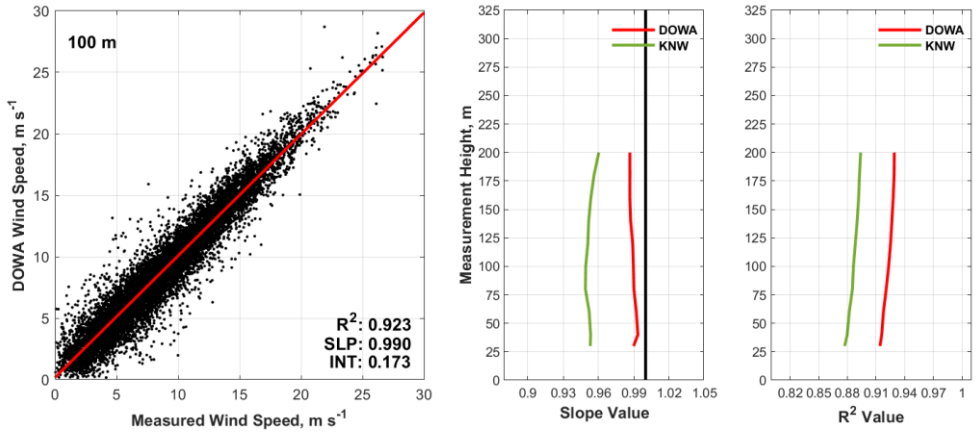

Figure 13 Same as Figure 8 except at HKZb.

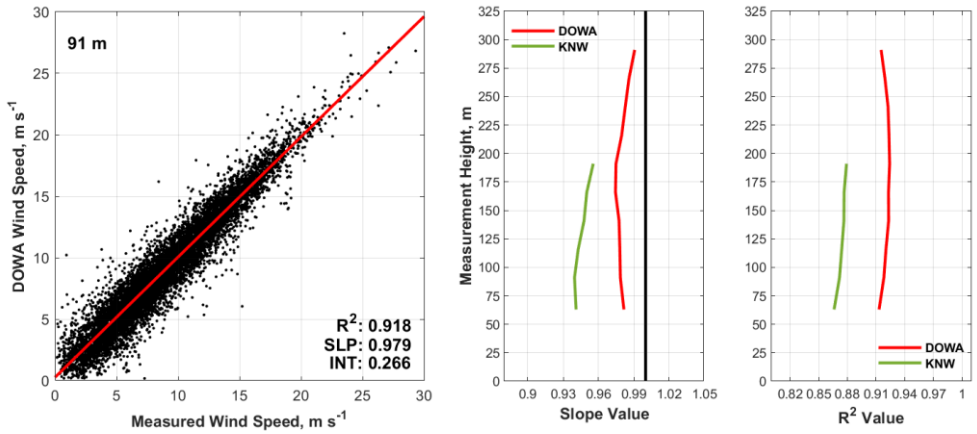

Figure 14 Same as Figure 8 except at EPL.

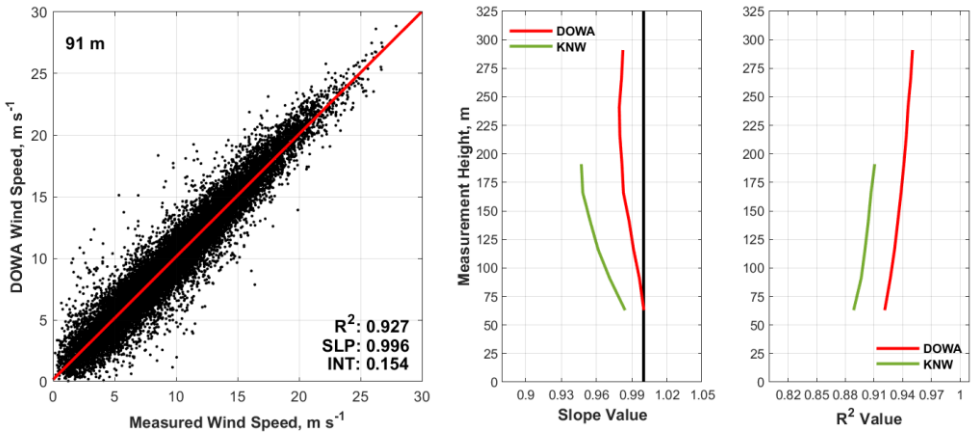

Figure 15 Same as Figure 8 except at LEG.

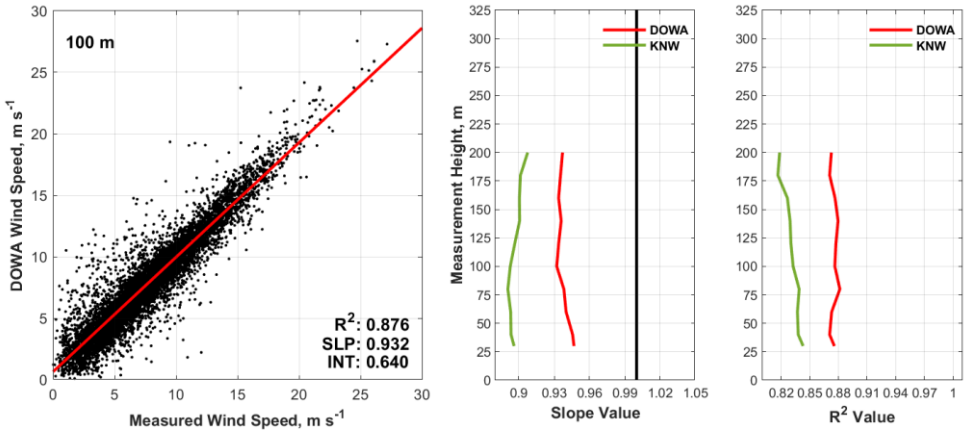

Figure 16 Same as Figure 8 except at BWFZ1.

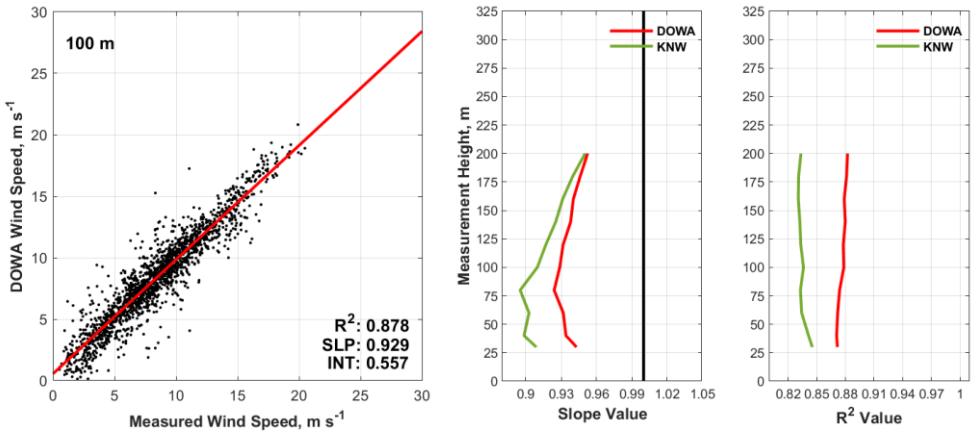

Figure 17 Same as Figure 8 except at BWFZ2.

3.1.2 Validation of the DOWA against offshore meteorological masts

The same analysis performed in Section 3.1.1 was applied to the instrumented meteorological tower measurements at MMIJ and OWEZ; Figures 18 and 19 and Table 6 correspond to this analyses. Comparison to the instrumented meteorological tower measurements at these locations indicates—similar to the comparison to LiDAR wind speeds—improved hourly wind speed correlation within the DOWA.

Linear least-squares regression between the DOWA and the instrumented meteorological tower measurements at MMIJ produced a slope and R^2 value, respectively, of 0.99 and 0.93 at 27m, 0.99 and 0.94 at 58m, and 0.99 and 0.94 at 85m. Alternatively, linear least-squares regression between the KNW-atlas and the instrumented meteorological tower measurements at MMIJ produced a slope and R^2 value, respectively, of 0.98 and 0.91 at 27m, 0.97 and 0.91 at 58m, and 0.97 and 0.91 at 85m. The minimum slope value produced by the DOWA at OWEZ was 0.98 at 70m, wherein the R^2 value was 0.90. At this height at OWEZ, the KNW-atlas produced a slope value of 0.96 and an R^2 value of 0.87. These results indicate that compared to the KNW-atlas hourly wind speed correlation was improved within the DOWA.

Table 6 The slope, y-intercept, and R^2 values derived from performing linear least-squares regression between the wind atlas and LiDAR wind speeds.

Measurement Location Identifier (hgt)	Slope Value (KNW | DOWA)		Y-Intercept Value (KNW | DOWA)		R^2 Value (KNW | DOWA)	
MMIJ (85 m)	0.97	0.99	0.28	0.20	0.91	0.94
OWEZ (116 m)	0.96	0.99	0.53	0.43	0.89	0.92

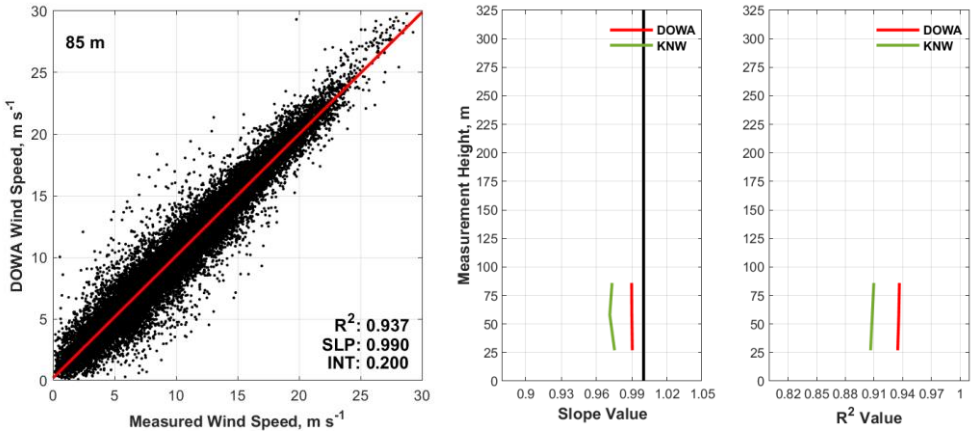

Figure 18 (Left column) Scatterplot of the DOWA and LiDAR wind speeds at MMIJ. (Right column) Vertical differences in the value of the linear least-squares regression slope and R^2.

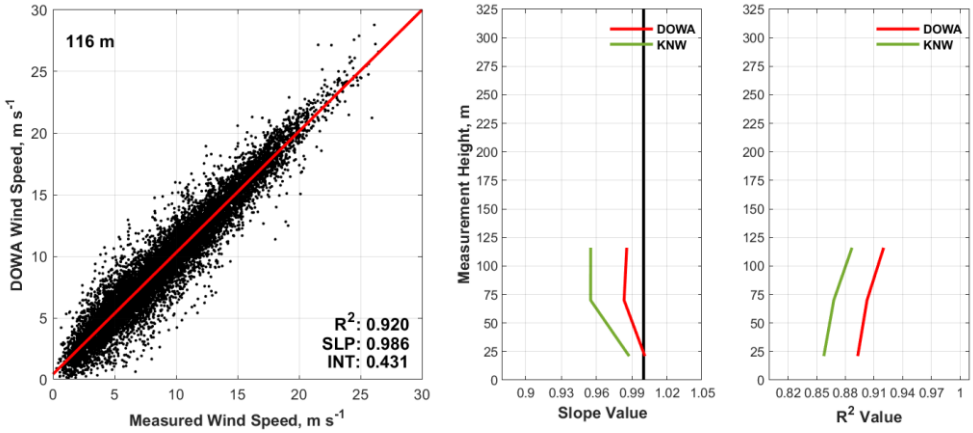

Figure 19 Same as Figure 18 except at OWEZ.

3.2 Seasonal and diurnal average wind speeds

3.2.1 Validation of the DOWA against offshore LiDAR

The ability of the KNW-atlas and the DOWA to resolve seasonal and diurnal average wind speeds at each LiDAR measurement location is demonstrated in Figures 20 through 29. Seasonal performance was quantified by determining the calendar month mean wind speed of the collocated datasets and then determining the average of these calendar month values at each measurement height and location examined. Seasonal (i.e. calendar month) LiDAR data availability is provided in the left subplot of Figures 20 through 29; with the quality control measures applied, there are very few months wherein monthly LiDAR data availability was 100% (data availability can be as low as 30.2% [December BWFZ1]). The conclusion of this analysis is that both wind atlases were able to reliably discern seasonal wind speed variability. The calendar-month mean wind speed bias at all measurement locations examined was -0.062m/s (a slight overestimation) for the DOWA and 0.025m/s (a slight underestimation) for the KNW-atlas. In an absolute sense, the largest calendar-month mean wind speed DOWA bias (-0.29m/s) was observed in December, whereas the smallest calendar-month mean wind speed DOWA bias (0.00034m/s) was observed in August. Even when defined relative to the magnitude of the calendar-month mean wind speed, the smallest calendar-month mean wind speed DOWA bias was observed in August (0.024% error) and the largest calendar-month mean wind speed DOWA bias was observed in December (-2.78% error). There was no strong evidence to suggest degraded DOWA performance within any specific season.

The representation of the diurnal cycle within the DOWA is significantly improved relative to that resolved within the KNW-atlas. These improvements were expected because of the changes in how the DOWA was made (i.e. additional data assimilation and the removal of cold starts). In order to demonstrate these improvements, the mean (μ) and standard deviation (σ) of the hourly wind speed bias at 00:00 UTC, 06:00 UTC, 12:00 UTC, and 18:00 UTC at each LiDAR measurement location are provided in Tables 7 and 8. The mean hourly wind speed bias considering all LiDAR locations was -0.053m/s for the DOWA and 0.022m/s for the KNW-atlas. However, the mean hourly wind speed bias does not indicate whether either wind atlas properly resolved the diurnal cycle in wind speed. For instance, a distribution can have large residuals yet still exhibit a mean bias of zero. Therefore, the σ value of the hourly wind speed bias was also examined in order to more thoroughly quantify the extent to which the wind atlases can resolve the diurnal cycle in wind speed. At each LiDAR measurement location and wind atlas forecast hour (i.e. 00:00 UTC, 01:00 UTC, etc.), the DOWA reduced the σ value of the hourly wind speed bias. On average, the σ value of the hourly wind speed bias was reduced by 0.26m/s (16.99%) from a mean value of 1.53m/s within the KNW-atlas to a mean value of 1.27m/s within the DOWA.

Table 7 Mean hourly wind speed bias (i.e. $WS_{meas} - WS_{atlas}$) at 00:00 UTC, 06:00 UTC, 12:00 UTC, and 18:00 UTC for each LiDAR measurement location.

Measurement Location Identifier (hgt)	**μ Bias (m/s) at 00:00 UTC (KNW | DOWA)**		**μ Bias (m/s) at 06:00 UTC (KNW | DOWA)**		**μ Bias (m/s) at 12:00 UTC (KNW | DOWA)**		**μ Bias (m/s) at 18:00 UTC (KNW | DOWA)**	
MMIJ (90 m)	-0.22	-0.08	-0.28	-0.10	-0.21	-0.23	-0.24	-0.05
K13a (91 m)	-0.44	-0.21	-0.29	-0.19	-0.19	-0.34	-0.41	-0.25
HKNa (100 m)	-0.35	-0.23	-0.08	0.01	0.06	-0.18	-0.23	0.97
HKNb (100 m)	-0.35	-0.15	-0.07	0.08	0.05	-0.19	-0.21	0.88
HKZa (100 m)	-0.28	-0.16	-0.32	-0.14	-0.12	-0.20	-0.31	-0.03
HKZb (100 m)	-0.33	-0.20	-0.34	-0.13	-0.16	-0.20	-0.33	-0.03
EPL (91 m)	-0.29	-0.17	-0.22	-0.06	-0.19	-0.16	-0.18	0.06
LEG (91 m)	-0.24	-0.16	-0.36	-0.19	-0.19	-0.17	-0.19	-0.10
BWFZ1 (100 m)	-0.28	0.05	-0.23	-0.14	-0.27	-0.08	-0.25	-0.07
BWFZ2 (100 m)	-0.33	0.04	-0.28	-0.05	-0.20	0.10	-0.13	-0.25

Table 8 Standard deviation of the hourly wind speed bias at 00:00 UTC, 06:00 UTC, 12:00 UTC, and 18:00 UTC for each LiDAR measurement location.

Measurement Location Identifier (hgt)	**σ Bias (m/s) at 00:00 UTC (KNW | DOWA)**		**σ Bias (m/s) at 06:00 UTC (KNW | DOWA)**		**σ Bias (m/s) at 12:00 UTC (KNW | DOWA)**		**σ Bias (m/s) at 18:00 UTC (KNW | DOWA)**	
MMIJ (90 m)	1.57	1.24	1.49	1.25	1.52	1.23	1.67	1.30
K13a (91 m)	1.51	1.24	1.54	1.26	1.53	1.24	1.66	1.27
HKNa (100 m)	1.64	1.47	1.26	0.98	1.63	1.23	2.00	1.43
HKNb (100 m)	1.67	1.44	1.27	1.03	1.48	1.17	1.91	1.43
HKZa (100 m)	1.68	1.28	1.51	1.17	1.52	1.26	1.86	1.39
HKZb (100 m)	1.68	1.28	1.53	1.20	1.48	1.22	1.84	1.35
EPL (91 m)	1.65	1.33	1.48	1.18	1.46	1.21	1.79	1.39
LEG (91 m)	1.59	1.38	1.57	1.28	1.47	1.24	1.83	1.41
BWFZ1 (100 m)	1.68	1.45	1.49	1.31	1.50	1.39	1.94	1.44
BWFZ2 (100 m)	2.10	1.43	1.22	1.65	1.33	1.05	1.94	1.46

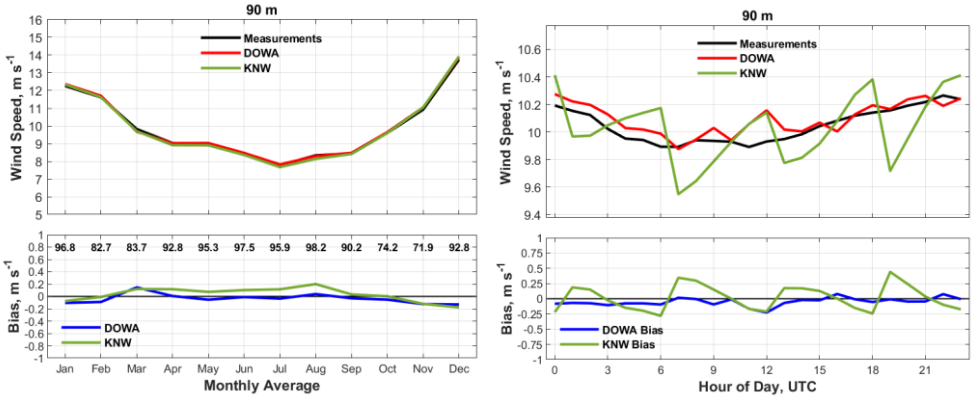

Figure 20 (Top Subplots) Calendar-month mean (left column) and hourly mean (i.e. diurnal) (right column) LiDAR and wind atlas wind speeds at MMIJ. Numerical values located in the bottom-left subplot indicate the data availability percentage for that calendar month. (Bottom Subplots) Wind atlas wind speed bias (i.e. $WS_{meas} - WS_{atlas}$).

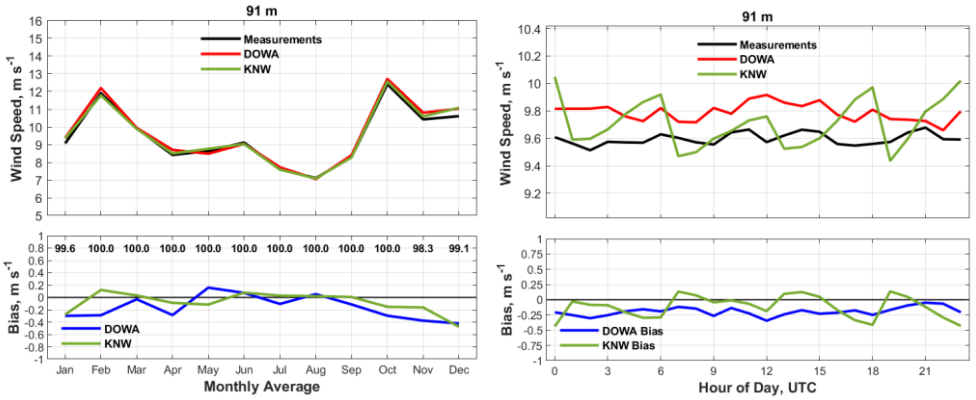

Figure 21 Same as Figure 20 except at K13a.

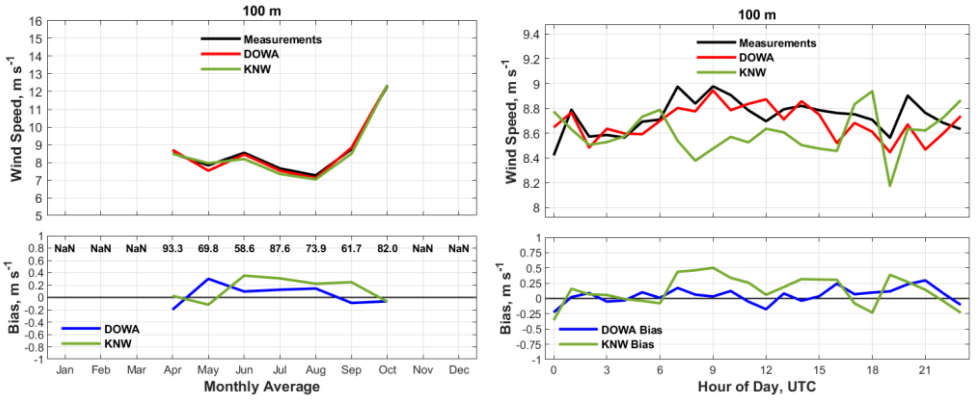

Figure 22 Same as Figure 20 except at HKNa.

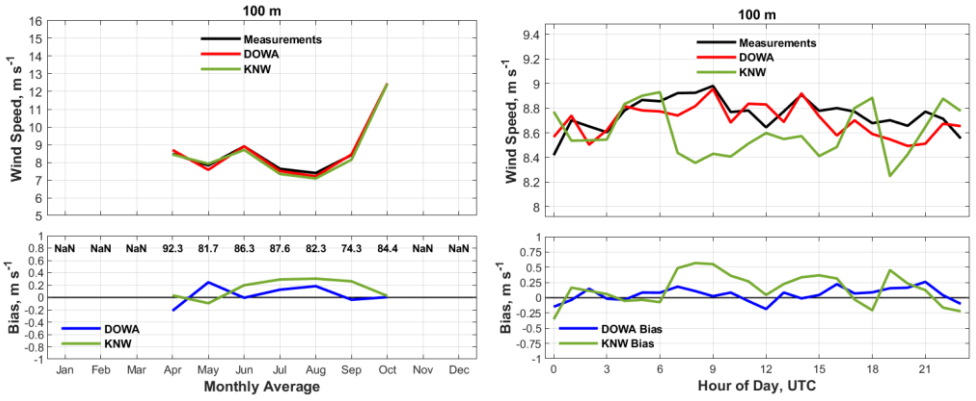

Figure 23 Same as Figure 20 except at HKNb.

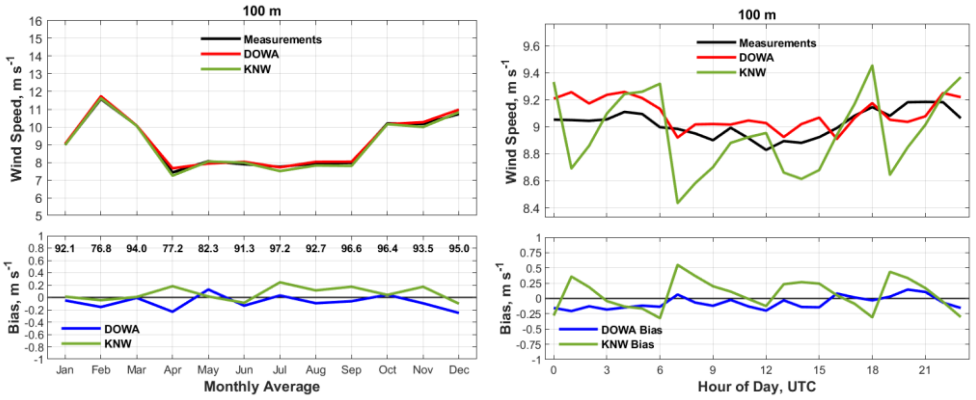

Figure 24 Same as Figure 20 except at HKZa.

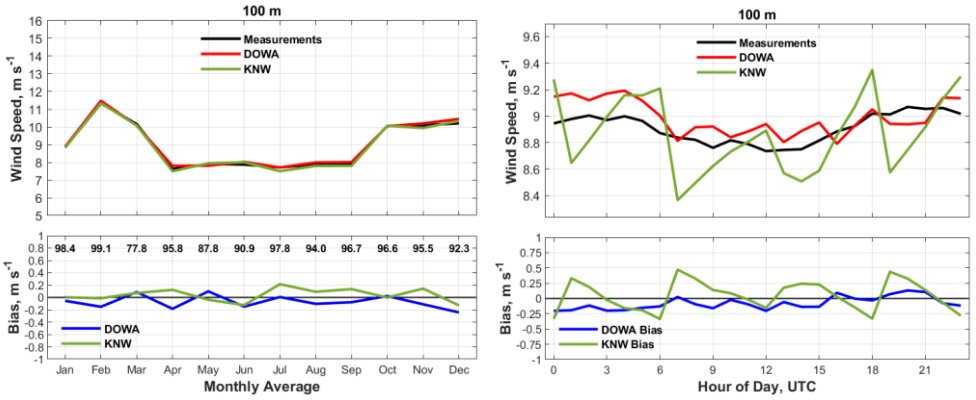

Figure 25 Same as Figure 20 except at HKZb.

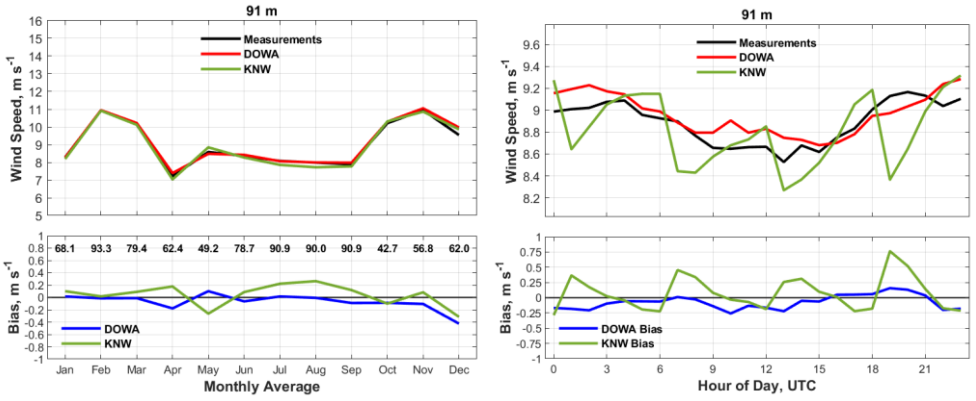

Figure 26 Same as Figure 20 except at EPL.

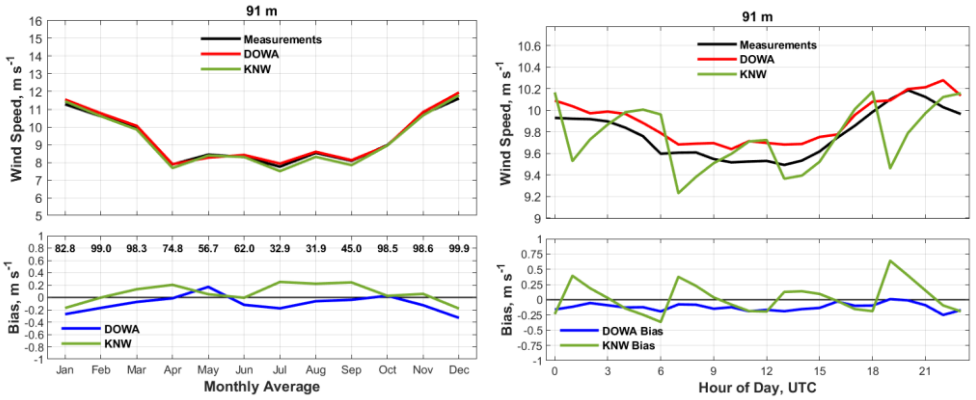

Figure 27 Same as Figure 20 except at LEG.

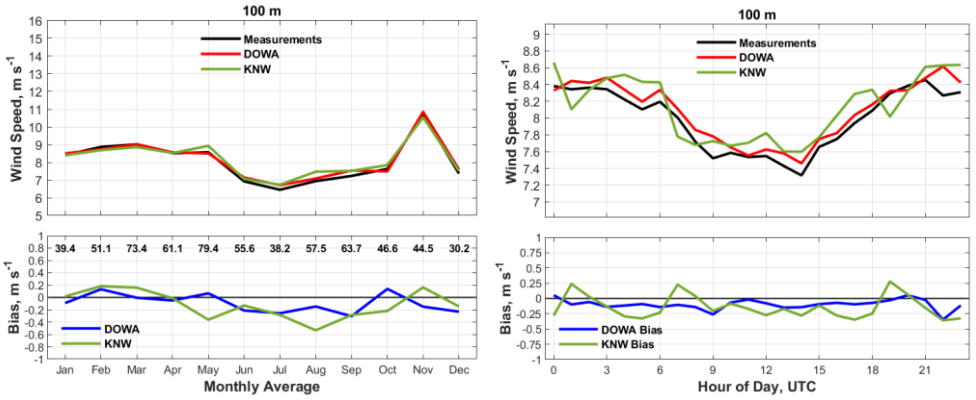

Figure 28 Same as Figure 20 except at BWFZ1.

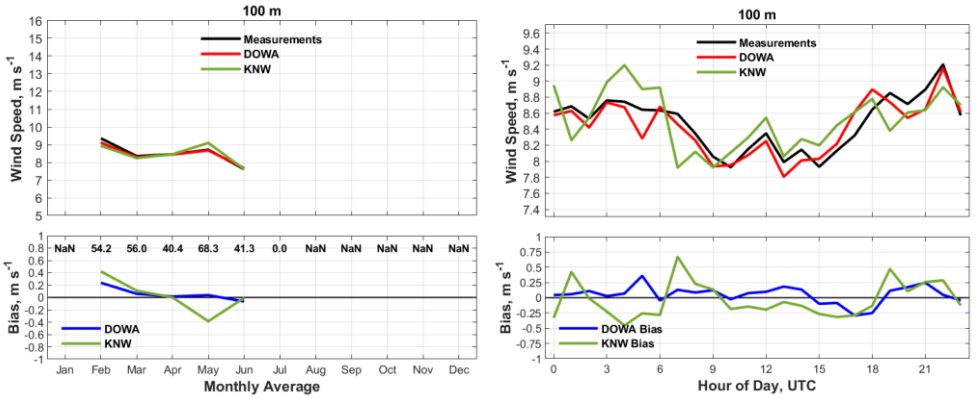

Figure 29 Same as Figure 20 except at BWFZ2.

3.2.2 Validation of the DOWA against offshore meteorological masts

Seasonal (i.e. calendar-month average) and diurnal (i.e. hourly average) wind speeds were compared to instrumented meteorological mast measurements at both MMIJ (Figure 30) and OWEZ (Figure 31). Seasonal (i.e. calendar month) meteorological mast data availability is provided in the left subplot of Figures 30 and 31; with the quality control measures applied, there are very few months wherein monthly meteorological mast data availability was 100%. Similar to the conclusions drawn from comparison to offshore LiDAR, both the KNW-atlas and the DOWA were able

to reliably discern seasonal wind speeds. At MMIJ, the KNW-atlas exhibited a calendar-month mean wind speed bias of 0.017m/s at 27m, 0.0083m/s at 58m, and 0.00024m/s at 85m, while the DOWA exhibited a calendar-month mean wind speed bias of -0.13m/s at 27m, -0.10m/s at 58m, and -0.089m/s at 85m. However, at OWEZ, both the KNW-atlas and the DOWA slightly overestimated the calendar-month mean wind speed values.

The representation of the diurnal cycle was enhanced within the DOWA compared to that within the KNW-atlas. However, this improvement is not demonstrated by a reduction in μ of the hourly wind speed bias (Table 9), but instead a significant reduction in σ of the hourly wind speed bias (Table 10). At MMIJ, the mean σ value of the hourly wind speed bias across all hourly forecast intervals was 1.10m/s at 27m, 1.18m/s at 58m, and 1.24m/s at 85m within the DOWA, and was 1.31m/s at 27m, 1.40m/s at 58m, and 1.46m/s at 85m within the KNW-atlas. At OWEZ, the DOWA on average reduced the σ value of the hourly wind speed bias by 0.18m/s at 21m, 0.19m/s at 70m, and 0.22m/s at 116m. These results indicate that the DOWA reduces the magnitude of the non-physical jumps and therefore provides a more accurate representation of the diurnal cycle in wind speed.

Table 9 Mean hourly wind speed bias (i.e. $WS_{meas} - WS_{atlas}$) at 00:00 UTC, 06:00 UTC, 12:00 UTC, and 18:00 UTC for each mast measurement location.

Measurement Location Identifier (hgt)	**μ Bias (m/s) at 00:00 UTC (KNW | DOWA)**		**μ Bias (m/s) at 06:00 UTC (KNW | DOWA)**		**μ Bias (m/s) at 12:00 UTC (KNW | DOWA)**		**μ Bias (m/s) at 18:00 UTC (KNW | DOWA)**	
MMIJ (85 m)	-0.26	-0.15	-0.29	-0.10	-0.21	-0.27	-0.26	-0.13
OWEZ (116 m)	-0.41	-0.39	-0.33	-0.20	-0.43	-0.36	-0.48	-0.41

Table 10 Standard deviation of the hourly wind speed bias at 00:00 UTC, 06:00 UTC, 12:00 UTC, and 18:00 UTC for each mast measurement location.

Measurement Location Identifier (hgt)	**σ Bias (m/s) at 00:00 UTC (KNW | DOWA)**		**σ Bias (m/s) at 06:00 UTC (KNW | DOWA)**		**σ Bias (m/s) at 12:00 UTC (KNW | DOWA)**		**σ Bias (m/s) at 18:00 UTC (KNW | DOWA)**	
MMIJ (85 m)	1.53	1.22	1.46	1.19	1.47	1.14	1.69	1.31
OWEZ (116 m)	1.59	1.40	1.54	1.33	1.68	1.32	1.80	1.40

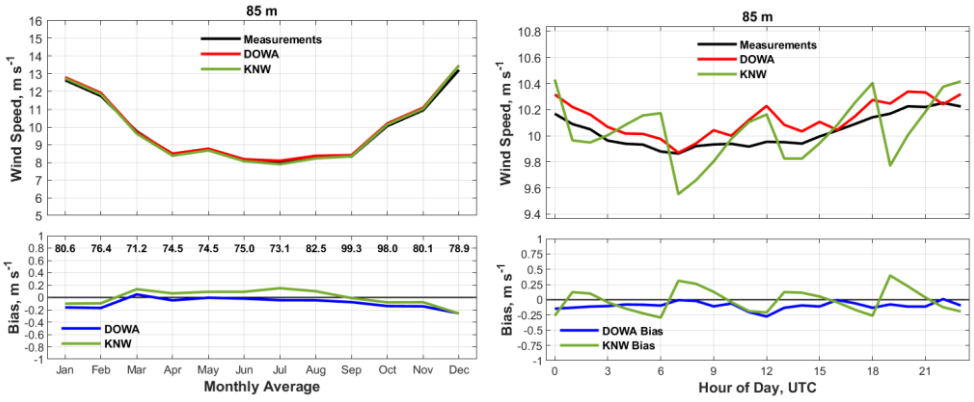

Figure 30 (Top Subplots) Calendar-month mean (left column) and hourly (i.e. diurnal) (right column) average LiDAR and wind atlas wind speeds at MMIJ. Numerical values located in the bottom-left subplot indicate the data availability percentage for that calendar month. (Bottom Subplots) Wind atlas wind speed bias (i.e. $WS_{meas} - WS_{atlas}$).

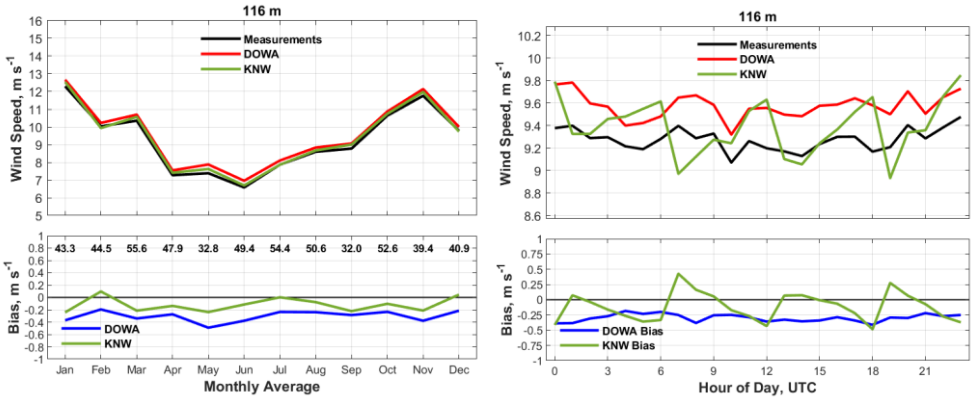

Figure 31 Same as Figure 30 except at OWEZ.

3.3 Weibull distribution at multiple heights

A two-parameter Weibull distribution can be used to reasonably depict variations in wind speed (i.e. the wind speed distribution) at a location (Burton et al. 2011; Rehman et al. 2012; Genc et al. 2005). This is why wind energy industry software and applications, such as the Wind Atlas Analysis and Applications Program (WAsP), often use the Weibull distribution to model the wind speed frequency distribution. As wind turbine technologies advance and wind energy extraction occurs at increasingly higher altitudes, how the Weibull distribution varies with height and how the wind atlases capture these vertical changes is increasingly important.

Methods established by Wieringa and Rijkoord (1983) and previously used to validate the KNW-atlas (Stepek et al. 2015) were used to determine the Weibull fit at each available measurement height and measurement location. A wind speed bin size of 0.5 m/s was used to determine the Weibull fit. Using this method, the Weibull parameters are defined by,

$$\ln(-\ln[1 - F(U)]) = k(\ln U) - k \ln A,$$

where $F(U)$ is the cumulative Weibull distribution function (i.e. the chance of exceeding wind speed U), k is the Weibull shape parameter, and A is the Weibull scale parameter. The parameter A is proportional to the mean wind speed of the distribution and the parameter k depicts the shape of the distribution. The value of *k* is inversely proportional to the spread of the wind speed distribution. Therefore, large *k* values indicate less variation in the wind.

3.3.1 Validation of the DOWA against offshore LiDAR

A Weibull distribution was fit to wind speed data (LiDAR and wind atlas) at each LiDAR measurement height. The left column of Figures 32 through 41 provides these fits for the LiDAR measurement height nearest 100m and the right column of these figures demonstrates differences in *A* and *k* with height. The data collection period at both HKN and BWFZ2 was shorter than one year; therefore, the Weibull fit at these measurement locations will not be representative of the annual wind conditions. Furthermore, the Weibull parameters will also be impacted by the wind direction filtering that was imposed to limit neighboring wind farm wake effects. Therefore, the Weibull distribution parameters presented below were purely developed for comparison purposes and should not be interpreted as representative of the measurement site's wind climate.

The values of *A* and *k* at the LiDAR measurement heights nearest 100m, 200m, and at the maximum LiDAR measurement height (MLMH) in excess of 200m, are provided in Tables 11 and 12 for each LiDAR measurement location. Because *A* is proportional to mean wind speed, the value of *A* tends to increase with height. In general, both wind atlases were able to resolve vertical changes in *A* with height. At the LiDAR measurement height nearest 100m, the DOWA exhibited a mean *A* bias of -0.071m/s (overestimation) and the KNW-atlas exhibited a mean *A* bias of only 0.0073m/s (underestimation). Near 200m, both the DOWA and the KNW-atlas overestimated the value of *A*; the DOWA exhibited a mean *A* bias of -0.089m/s and the KNW-atlas exhibited a mean *A* bias of -0.084m/s. Furthermore, at the MLMH, the mean *A* bias was -0.080m/s within the DOWA. The main conclusion of this analysis is that even without incorporating a uniform shear-correction factor—as was done in the KNW-atlas—the DOWA performed similar to the KNW-atlas in depicting vertical changes in *A* with height.

Wind is slowed by friction at the surface. Therefore, the range of possible wind speeds is generally smaller near the surface than aloft, which is why the value of *k* typically decreases with height. Offshore, sea surface roughness (i.e. a friction source) is correlated to the near-surface wind conditions (Hersbach 2011; Kudryavstev and Makin 2007). As near-surface wind speeds increase, sea surface roughness also increases (i.e. the sea surface is rougher at higher wind speeds). Therefore, although near-surface wind speeds drive sea surface roughness, sea surface roughness also inhibits extreme wind speeds. The effect of sea surface roughness on wind speed decreases with height offshore, allowing higher wind speeds to develop aloft while near-surface wind speed continue to be damped by sea surface roughness. This means that the value of *k* (inversely proportional to the range of possible wind speeds) should decrease with height. Both the KNW-atlas and the DOWA were able to reliably denote the offshore decrease in *k* with height. At the LiDAR measurement location nearest 100m, the KNW-atlas exhibited a mean *k* bias of 0.0025 (underestimation) and the DOWA exhibited a mean *k* bias of 0.023 (underestimation). The wind atlases continue to slightly underestimate the value of *k* at the LiDAR measurement height nearest 200m; the KNW-atlas underestimated *k* by a mean value of 0.0040, while the DOWA underestimated the value of *k* by a mean value of 0.091. At the MLMH, the DOWA underestimate the value of *k* by a mean value of 0.038.

Table 11 The value of *A* at the LiDAR measurement height nearest 100 m, 200 m, and at the MLMH.

Measurement Location Identifier and MLMH (if applicable)	**Weibull Scale Parameter (m/s) Nearest 100 m (Meas. | KNW | DOWA)**			**Weibull Scale Parameter (m/s) Nearest 200 m (Meas. | KNW | DOWA)**			**Weibull Scale Parameter (m/s) at the MLMH (hgt) (Meas. | KNW | DOWA)**		
MMIJ (315 m)	11.38	11.36	11.41	12.10	12.12	12.10	12.37	N/A	12.41
K13a (291 m)	10.79	10.94	11.02	11.54	11.70	11.65	11.76	N/A	11.90
HKNa	9.81	9.72	9.78	10.23	10.22	10.24	Same Height as 200 m		
HKNb	9.82	9.75	9.79	10.24	10.22	10.23	Same Height as 200 m		
HKZa	10.17	10.11	10.26	10.63	10.72	10.89	Same Height as 200 m		
HKZb	10.04	10.01	10.13	10.53	10.61	10.66	Same Height as 200 m		
EPL (291 m)	9.99	9.93	10.07	10.50	10.52	10.61	10.66	N/A	10.75
LEG (291 m)	11.05	11.07	11.21	12.15	12.01	12.21	12.98	N/A	13.04
BWFZ1	9.04	9.20	9.15	9.19	9.56	9.43	Same Height as 200 m		
BWFZ2	9.59	9.65	9.55	9.77	10.04	9.85	Same Height as 200 m		

Table 12 The value of *k* at the LiDAR measurement height nearest 100 m, 200 m, and at the MLMH.

Measurement Location Identifier and MLMH (if applicable)	Weibull Shape Parameter Nearest 100 m (Meas. | KNW | DOWA)			Weibull Shape Parameter Nearest 200 m (Meas. | KNW | DOWA)			Weibull Shape Parameter at the MLMH (hgt) (Meas. | KNW | DOWA)		
MMIJ (315 m)	2.19	2.14	2.15	2.06	2.02	2.03	1.99	N/A	1.93
K13a (291 m)	2.31	2.30	2.27	2.16	2.16	2.15	2.11	N/A	2.09
HKNa	2.20	2.17	2.16	2.12	2.09	2.10	Same Height as 200 m		
HKNb	2.13	2.14	2.12	2.07	2.06	2.06	Same Height as 200 m		
HKZa	2.15	2.13	2.11	2.03	2.03	2.02	Same Height as 200 m		
HKZb	2.15	2.13	2.11	2.04	2.03	2.02	Same Height as 200 m		
EPL (291 m)	2.19	2.15	2.16	2.05	2.02	2.05	2.03	N/A	1.97
LEG (291 m)	2.27	2.20	2.21	2.15	2.15	2.13	2.07	N/A	2.06
BWFZ1	2.11	2.21	2.15	2.02	2.10	2.06	Same Height as 200 m		
BWFZ2	2.37	2.46	2.39	2.30	2.30	2.30	Same Height as 200 m		

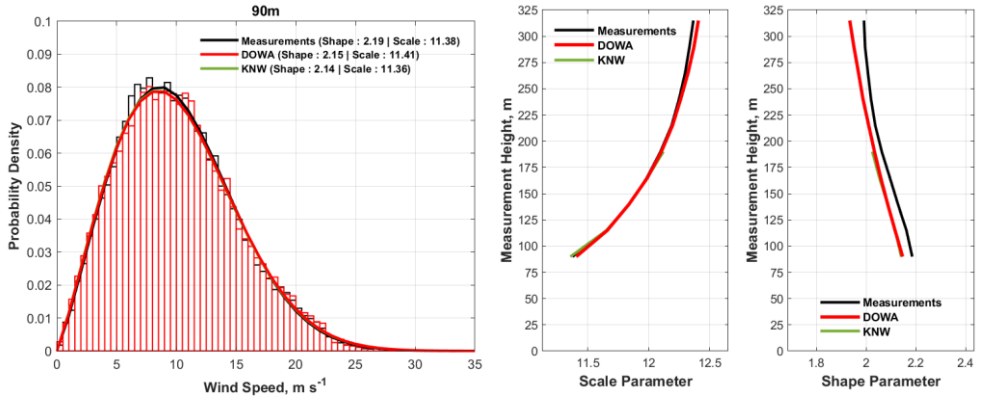

Figure 32 (Left column) The Weibull fit at the LiDAR measurement height nearest 100 m at MMIJ. (Right column) Vertical differences in *A* and *k* with height as defined by the LiDAR and two wind atlases.

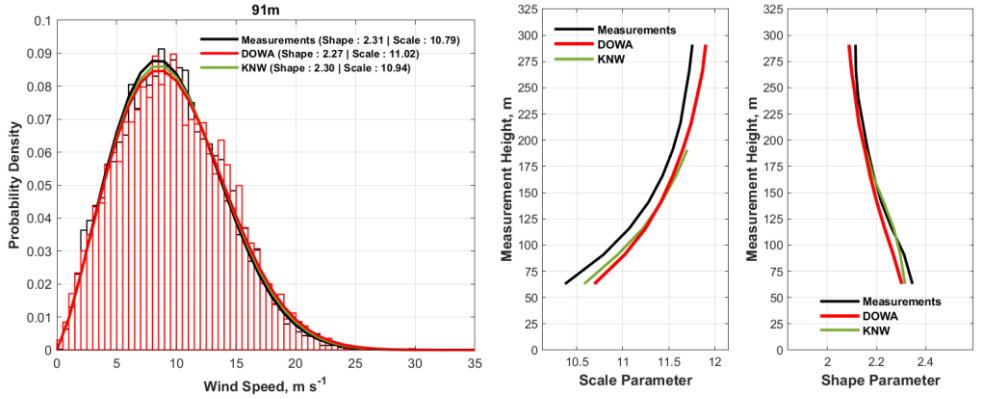

Figure 33 Same as Figure 32 except at K13a.

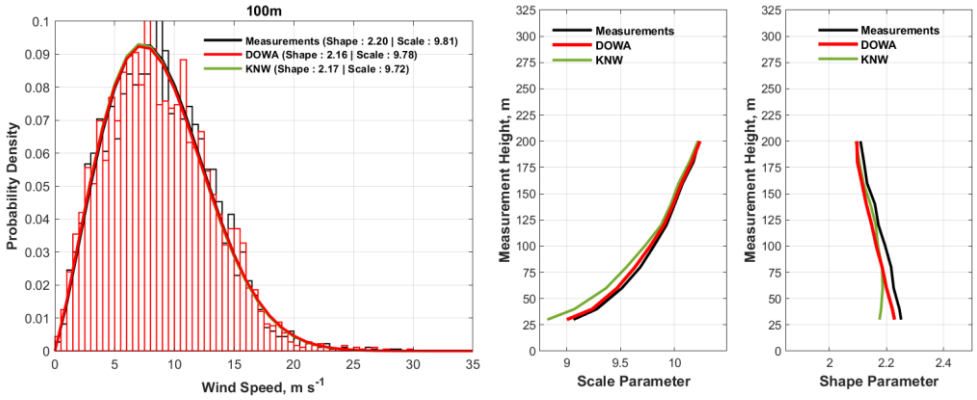

Figure 34 Same as Figure 32 except at HKNa.

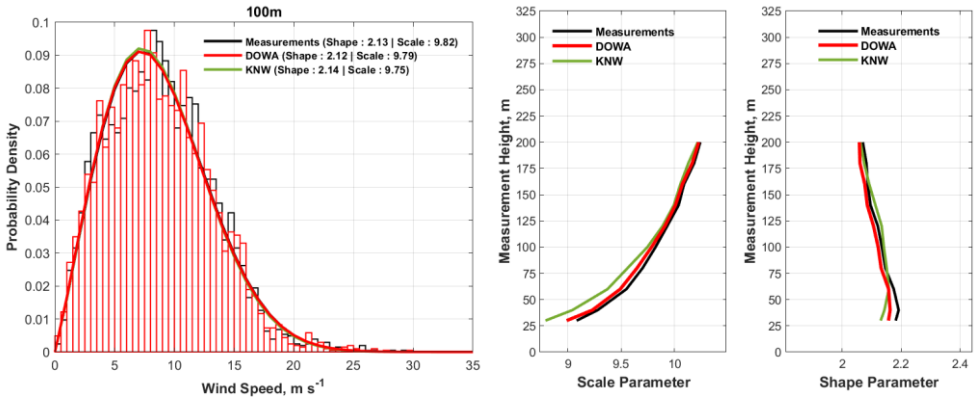

Figure 35 Same as Figure 32 except at HKNb.

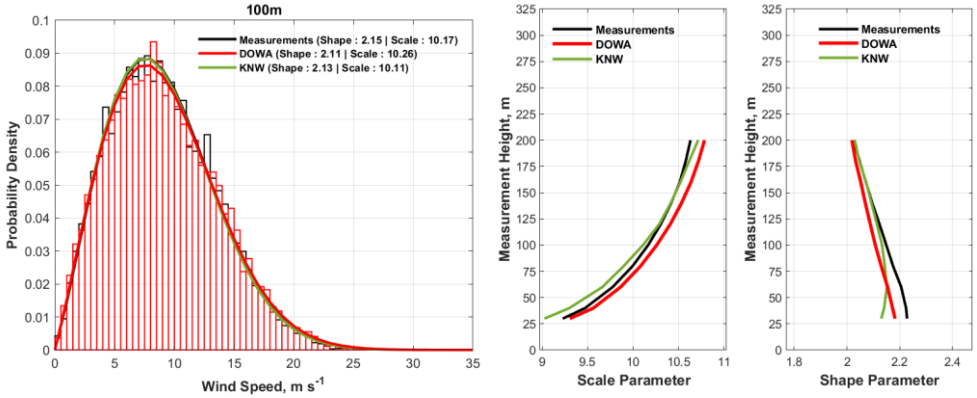

Figure 36 Same as Figure 32 except at HKZa.

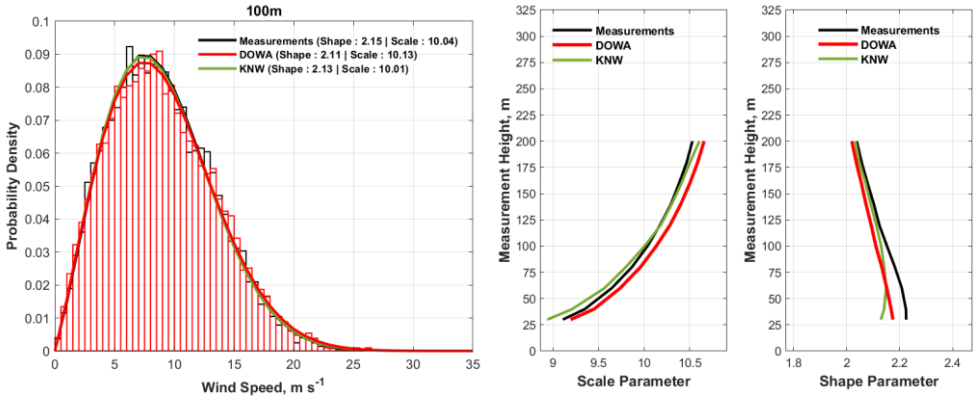

Figure 37 Same as Figure 32 except at HKZb.

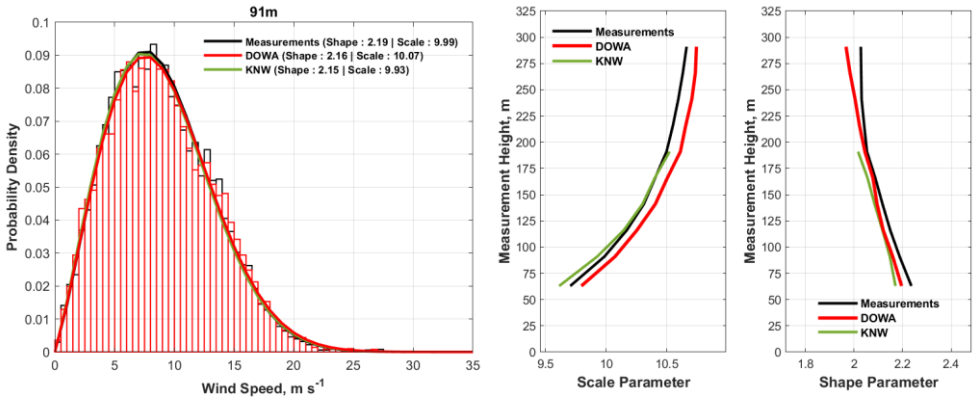

Figure 38 Same as Figure 32 except at EPL.

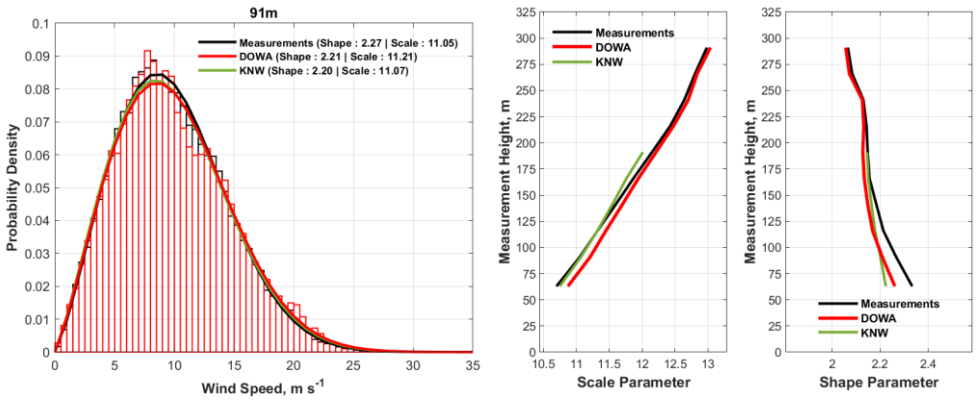

Figure 39 Same as Figure 32 except at LEG.

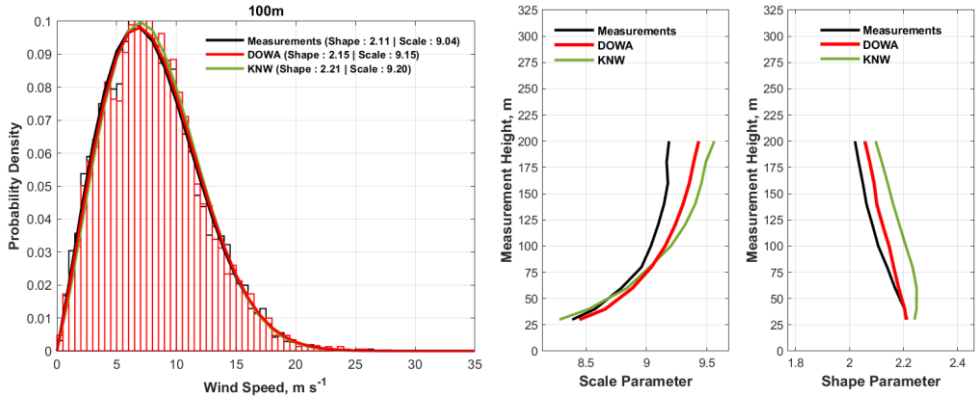

Figure 40 Same as Figure 32 except at BWFZ1.

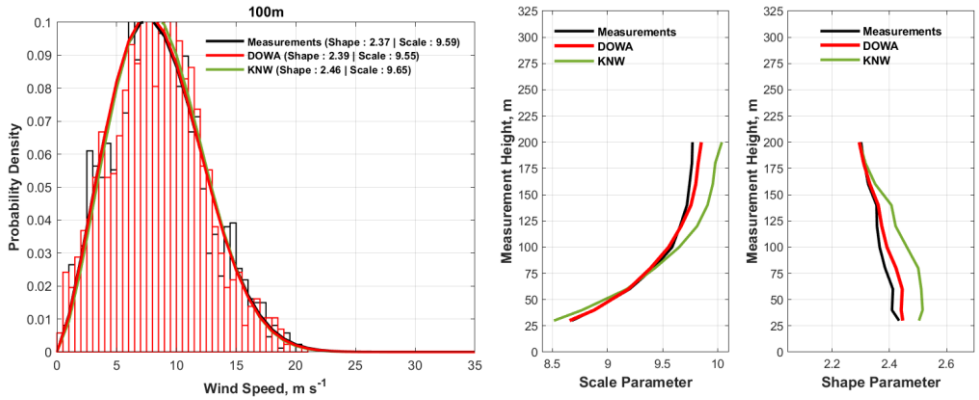

Figure 41 Same as Figure 32 except at BWFZ2.

3.3.2 *Validation of the DOWA against offshore meteorological masts*

The value of *A* and *k* was also derived from instrumented meteorological mast measurements at both MMIJ (Figure 42) and OWEZ (Figure 43) and compared to that produced by the two wind atlases. The corresponding statistics are provided in Table 13 for MMIJ and Table 14 for OWEZ. At both MMIJ and OWEZ, the wind atlases were able to reliably discern differences in *A* and *k* with height. The absolute bias in *A* at MMIJ did not exceed -0.13m/s (overestimation) within the DOWA and did not exceed 0.025m/s (underestimation) within the KNW-atlas. However, as expected based upon previous results, both wind atlases overestimated the value of *A* at OWEZ. With respect to discerning the value of *k*, the DOWA performed significantly better than the KNW-atlas at lower measurement heights. The mean *k* bias at MMIJ at 27m was 0.076 for the KNW-atlas and 0.027 for the DOWA. Similarly, the mean *k* bias at OWEZ at 21m was 0.10 for the KNW-atlas and -0.0052 for the DOWA. This discrepancy between the two wind atlas in their representation of *k* was smaller at higher elevations.

Table 13 Weibull parameters derived from MMIJ mast measurements, the KNW-atlas, and the DOWA.

Weibull Parameters	**Weibull Parameter (27m) (Meas. | KNW | DOWA)**			**Weibull Parameter (58m) (Meas. | KNW | DOWA)**			**Weibull Parameter (85m) (Meas. | KNW | DOWA)**		
Scale Parameter (m/s)	10.13	10.11	10.26	10.91	10.92	11.01	11.36	11.39	11.46
Shape Parameter	2.25	2.24	2.21	2.17	2.19	2.16	2.21	2.16	2.18

Table 14 Weibull parameters derived from OWEZ mast measurements, the KNW-atlas, and the DOWA.

Weibull Parameters	**Weibull Parameter (21m) (Meas. | KNW | DOWA)**			**Weibull Parameter (70m) (Meas. | KNW | DOWA)**			**Weibull Parameter (116m) (Meas. | KNW | DOWA)**		
Scale Parameter (m/s)	8.66	8.87	9.14	10.02	10.15	10.39	10.42	10.60	10.80
Shape Parameter	2.26	2.16	2.27	2.23	2.22	2.25	2.11	2.13	2.14

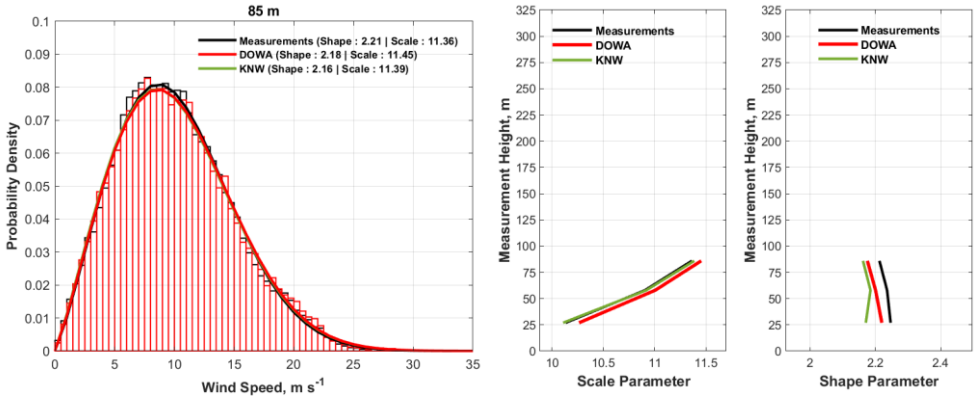

Figure 42 (Left column) The Weibull fit at the mast measurement height nearest 100 m for MMIJ. (Right column) Vertical differences in *A* and *k* with height as defined by the mast and two wind atlases.

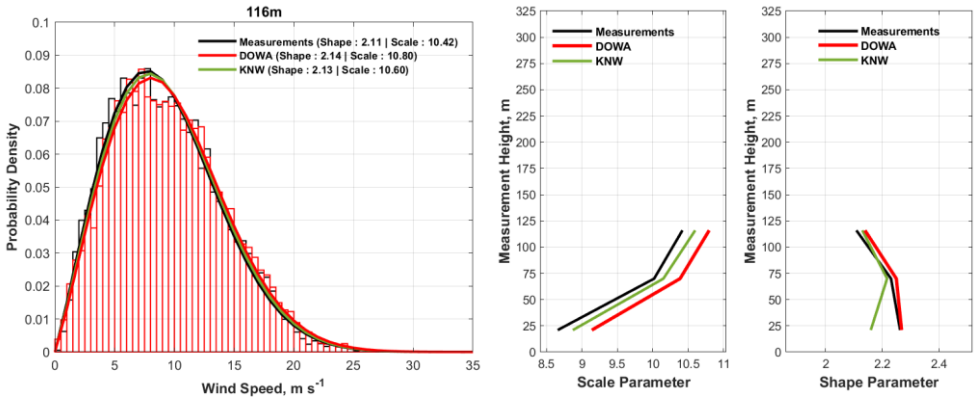

Figure 43 Same as Figure 42 except at OWEZ.

3.3.3 *Vertical profiles of wind speed*

Because *A* is proportional to mean wind speed, a section dedicated to vertical profiles of wind speed as defined by measurements (LiDAR and mast) and the wind atlases (the KNW-atlas and the DOWA) is not provided. However, figures depicting these vertical profiles of wind speed and the bias (μ and σ values) between the respective wind atlases and measurements are provided in Appendix C. Three observations can be made from these figures: (1) for all sites except for OWEZ the difference between the DOWA wind speed and the measurements is within measurement accuracy. Since Dutch offshore wind farm developments are further from shore than OWEZ, this is an excellent result. (2) the sign (i.e. +/-) of the DOWA wind speed bias generally does not change with height—while at some locations, the KNW-atlas will exhibit both a positive and negative wind sped bias depending upon the measurement height, and (3) at each measurement location and height, the σ value of the DOWA wind speed bias was less than that observed within the KNW-atlas.

3.4 Monthly and annual average wind speeds

3.4.1 Validation of the DOWA against offshore LiDAR

The ability of the KNW-atlas and the DOWA to resolve the monthly and annual average wind speeds at each LiDAR measurement location is demonstrated in Figures 44 through 52 and summarized in Tables 15 (monthly performance statistics) and 16 (annual performance statistics). Data availability is defined in these figures as the percentage of valid hourly measurements within the month or annual averaging period, and annual availability denotes the percentage of the calendar year wherein measurement occurred (i.e. the number of one-hour measurements divided by the number of hours in one year [i.e. 8760]).

Considering all LiDAR locations and comparable measurement heights (i.e. 90m $\leq$ h $\leq$ 200m), the μ value of the wind speed bias between the wind atlas and LiDAR mean monthly wind speeds was -0.070m/s (overestimation) for the DOWA and -0.019m/s for the KNW-atlas (overestimation). Although the KNW-atlas bias is smaller than that of the DOWA, the σ value of the wind speed bias was less for the DOWA (0.17m/s) than it was for the KNW-atlas (0.24m/s). This reduction in the value of σ was also evident at higher elevations (i.e. ~ 200m).

The μ value of the annual wind speed bias between the LiDAR and wind atlas wind speeds at the lidar measurement height nearest 100m was -0.085m/s (overestimation) in the DOWA and -0.015m/s (overestimation) in the KNW-atlas. Reduced monthly performance within both the KNW-atlas and the DOWA—such as that observed between July 2013 and May 2014 of Figure 44—was associated, in part, with periods of decreased data availability. All statistics were based upon the collocated datasets (i.e. wind atlas data was only considered when measurements were available).

Table 15 Performance of the KNW-atlas and the DOWA in resolving the monthly mean LiDAR wind speeds.

Measurement Location Identifier (hgt)	**μ Bias (m/s) (KNW-atlas | DOWA)**		**σ Bias (m/s) (KNW-atlas | DOWA)**	
MMIJ (90 m)	-0.02	-0.04	0.24	0.16
K13a (91 m)	-0.14	-0.20	0.18	0.20
HKNa (100 m)	0.16	0.09	0.20	0.14
HKNb (100 m)	0.16	0.09	0.16	0.12
HKZa (100 m)	0.08	-0.07	0.13	0.13
HKZb (100 m)	0.05	-0.08	0.13	0.12
EPL (91 m)	0.00	-0.09	0.21	0.16
LEG (91 m)	0.08	-0.10	0.21	0.19
BWFZ1 (100 m)	-0.11	-0.10	0.31	0.18
BWFZ2 (100 m)	-0.07	0.01	0.22	0.05

Table 16 Performance of the KNW-atlas and the DOWA in resolving the annual average LiDAR wind speeds. Further, the σ value of the annual wind speed bias was not provided because most measurement locations did not have a data collection period in excess of two years.

Measurement Location Identifier (hgt)	**μ Bias (m s^{-1}) (KNW-atlas | DOWA)**	
MMIJ (90 m)	-0.03	-0.06
K13a (91 m)	-0.17	-0.26
HKNa (100 m)	0.13	0.05
HKNb (100 m)	0.15	0.05
HKZa (100 m)	0.07	-0.07
HKZb (100 m)	0.05	-0.08
EPL (91 m)	0.07	-0.08
LEG (91 m)	0.01	-0.12
BWFZ1 (100 m)	-0.17	-0.12
BWFZ2 (100 m)	-0.03	0.047

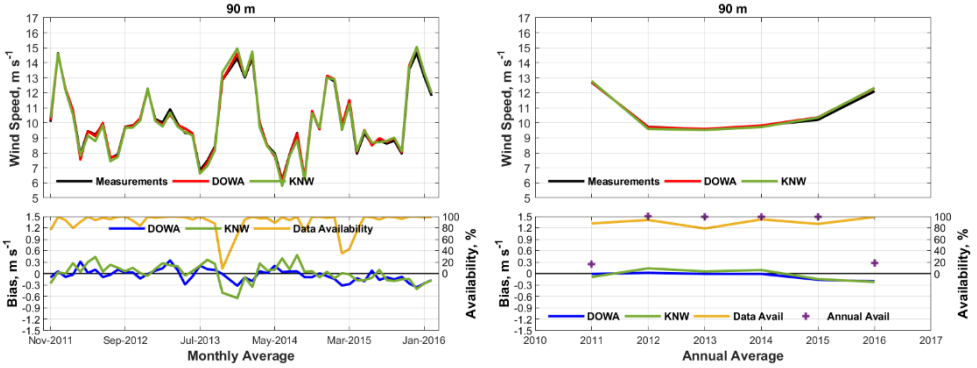

Figure 44 (Top Subplots) Monthly (left column) and annual (right column) average LiDAR and wind atlas wind speeds at MMIJ. (Bottom Subplots) Wind atlas wind speed bias (i.e. $WS_{meas} - WS_{atlas}$) as well as data and annual availability.

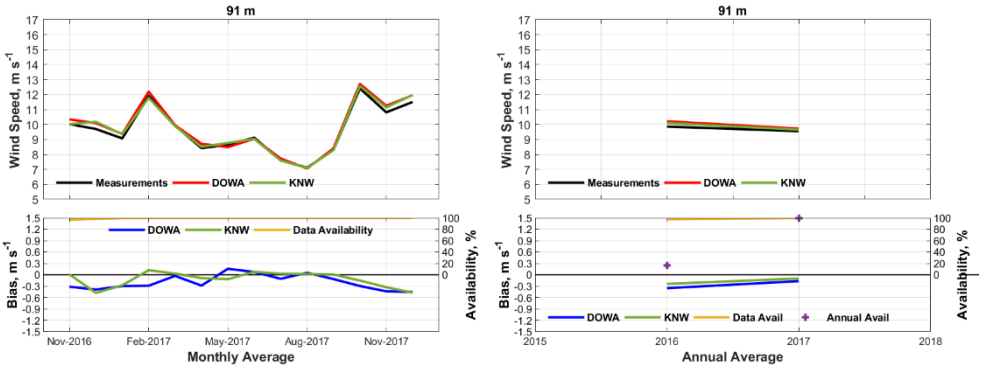

Figure 45 Same as Figure 44 except at K13a.

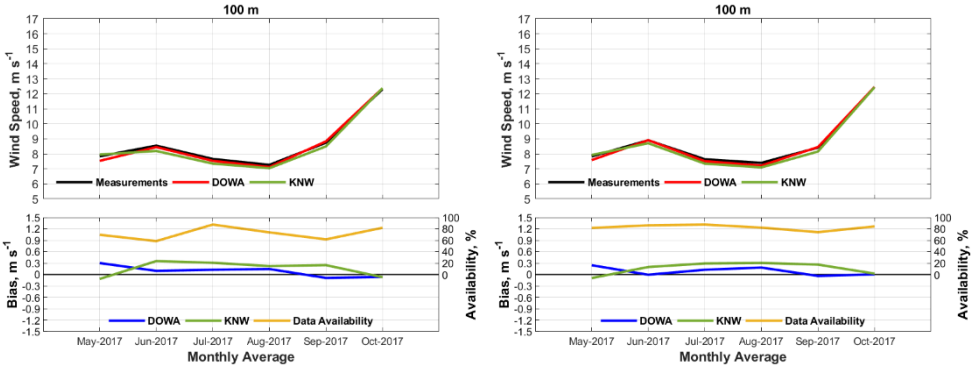

Figure 46 (Top Subplots) Monthly average LiDAR and wind atlas wind speeds at HKNa (left column) and HKNb (right column). (Bottom Subplots) Wind atlas wind speed bias (i.e. $WS_{meas} - WS_{atlas}$) and data availability. Annual average wind speed plots for HKNa and HKNb were not provided because the respective data records did not exceed one year.

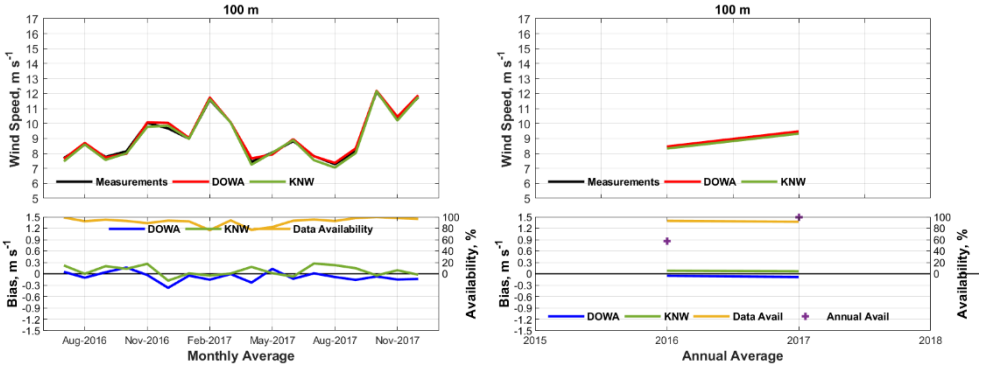

Figure 47 Same as Figure 44 except at HKZa.

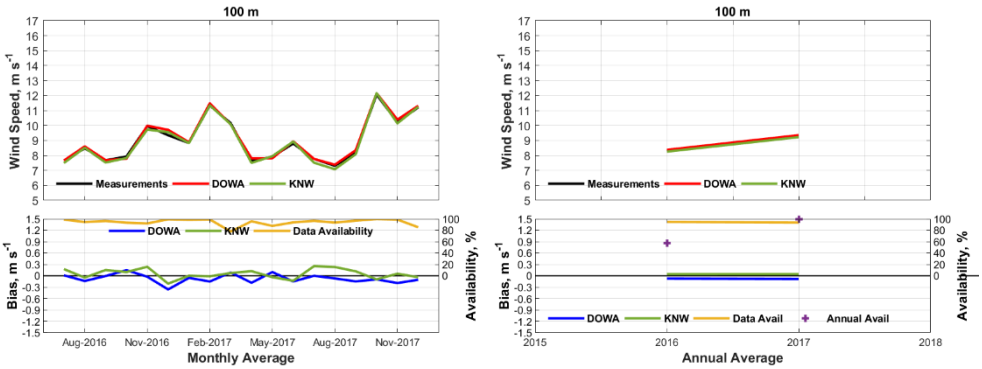

Figure 48 Same as Figure 44 except at HKZb.

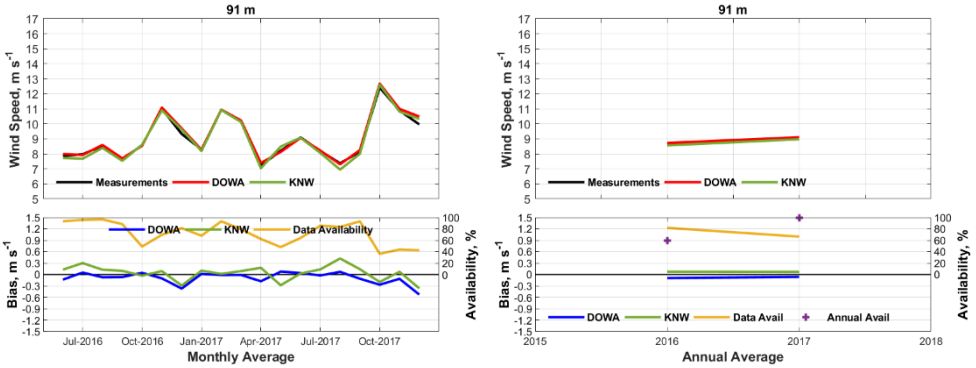

Figure 49 Same as Figure 44 except at EPL.

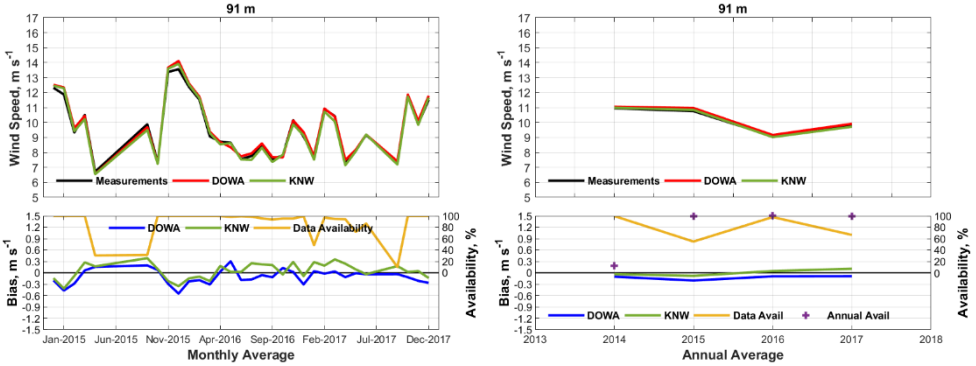

Figure 50 Same as Figure 44 except at LEG.

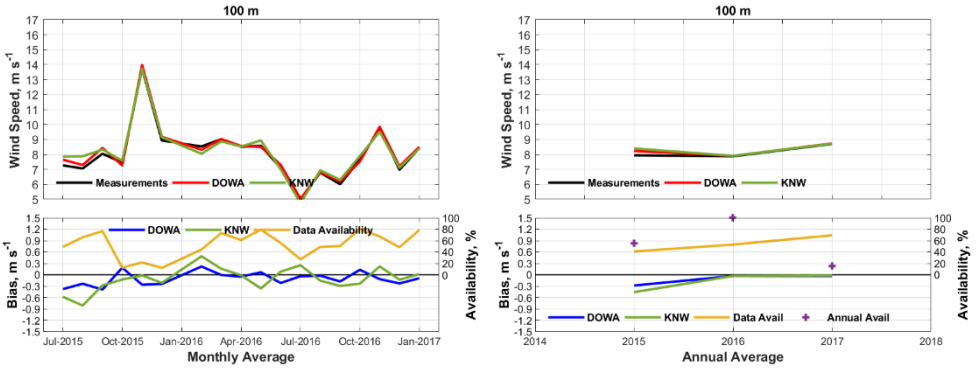

Figure 51 Same as Figure 44 except at BWFZ1.

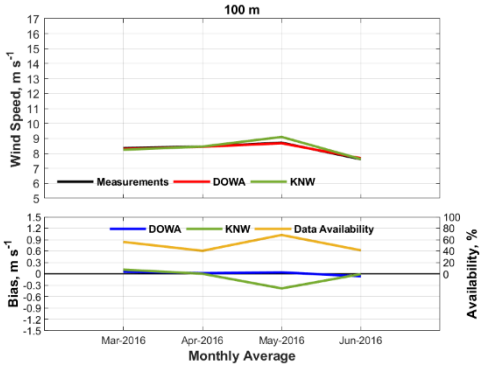

Figure 52 Same as Figure 44 (left column) except at BWFZ2. The annual average wind speed plot for BWFZ2 was not provided because the data record did not exceed one year.

3.4.2 Validation of the DOWA against offshore meteorological masts

Mean monthly and annual average wind atlas data were compared to instrumented meteorological mast measurements at both MMIJ and OWEZ. Representation of the mean monthly and annual average wind speeds by the two wind atlases is shown in Figure 53 for the comparison made at MMIJ and is shown in Figure 54 for the comparison made at OWEZ. Statistics summarizing wind atlas representation of the mean monthly and annual average wind speeds is provided in Tables 17 and 18. At both MMIJ and OWEZ, the DOWA overestimated the mean monthly and annual average wind speeds; however, performance in general was better at lower elevations. At MMIJ, the DOWA overestimated the monthly mean wind speeds by 0.13m/s at 27m, 0.11m/s at 58m, and 0.099m/s at 85m, while the KNW-atlas exhibited a mean monthly wind speed bias of -0.015m/s at 27m, -0.0061m/s at 70m, and 0.0061m/s at 85 m. At OWEZ, the DOWA overestimated the monthly mean wind speeds by 0.40m/s at 21m, 0.31m/s at 70m, and 0.30m/s at 116m, and the KNW-atlas overestimated the monthly mean wind speeds by 0.16m/s at 21m, 0.075m/s at 70m, and 0.11m/s at 116m. Similar overestimation of the wind speeds at OWEZ were noted within the DOWA when comparison was made to the annual average wind speeds.

OWEZ is the only measurement location examined where the KNW-atlas overestimated the monthly mean and annual average wind speeds. However, previous results suggest some issues with the anemometer with respect to accurately measuring wind speed gusts (van den Brink 2017). Because the wind farm was realized next to the measurement mast, the measurement sector was reduced significantly: measurements in the sector between 135 and 315 degrees are undisturbed.

Table 17 Performance of the KNW-atlas and the DOWA in resolving the monthly mean mast wind speeds.

Measurement Location Identifier (hgt)	**μ Bias (m/s) (KNW-atlas | DOWA)**		**σ Bias (m/s) (KNW-atlas | DOWA)**	
MMIJ (85 m)	0.01	-0.10	0.22	0.14
OWEZ (116 m)	-0.11	-0.30	0.16	0.12

Table 18 Performance of the KNW-atlas and the DOWA in resolving the annual average mast wind speeds.

Measurement Location Identifier (hgt)	μ Bias (m/s) (KNW-atlas | DOWA)	
MMIJ (85 m)	-0.00	-0.10
OWEZ (116 m)	-0.11	-0.30

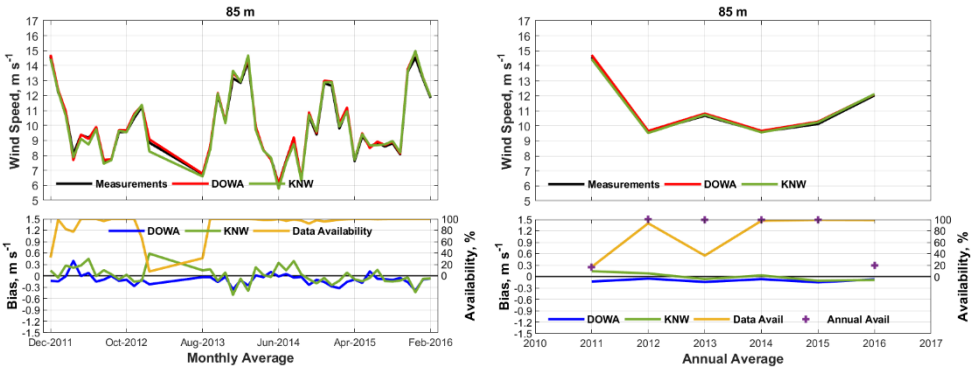

Figure 53 (Top Subplots) Monthly (left column) and annual (right column) average mast and wind atlas wind speeds at MMIJ. (Bottom Subplots) Wind atlas wind speed bias (i.e. $WS_{meas} - WS_{atlas}$) as well as data and annual availability.

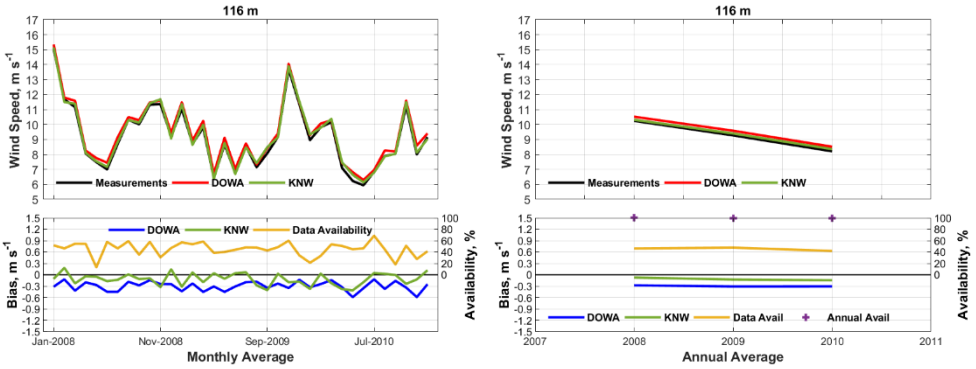

Figure 54 Same as Figure 53 except at OWEZ.

4 Validation of DOWA wind directions

Wind direction data was binned according to 30º sector bins (i.e. 0º to 30º, 30º to 60º, etc.) in order to conform with the wind direction validation analyses performed by Stepek et al. (2015). However, prior to binning the data, the wind directions were filtered as follows: (1) wind direction data was ignored if the 10-min mean wind speed was less than 4 m/s (near the cut-in wind speed of most modern wind turbines) and (2) wind direction sectors (shaded in the Figures presented in Section 4.1) were removed from analyses if they had the potential to contain a wind farm wake (see Appendix B.3). Because of this wind direction filtering, the wind direction distributions should not be interpreted as a site wind rose. Further, wind direction bin statistics were ignored if the bin midpoint (i.e. 15º is the midpoint for the 0º to 30º wind direction sector bin) resided within a wind direction sector that was removed from analyses to negate the wind farm wake effect.

4.1 Wind direction distributions and wind direction sector mean wind speeds

4.1.1 Validation of the DOWA against offshore LiDAR

LiDAR and wind atlas wind direction distributions at the LiDAR measurement height nearest 100 m are provided in the left column of Figures 55 through 64 for each LiDAR measurement location. Provided in the right column of these Figures is the wind direction bin mean wind speed. Both wind atlases were generally able to discern the measurement location wind direction distribution, but on average the wind direction distribution bias was less within the DOWA than within the KNW-atlas. The most significant discrepancies between the wind atlas and LiDAR wind direction distributions occurred at the border of adjacent wind direction bins—especially for the wind direction bins associated with the climatologically dominant wind directions. These discrepancies make sense; for instance, if a wind direction bin was aligned with the predominant wind direction, then just a few degree difference could significantly impact the probability density within the neighbouring wind direction bins.

Although not necessarily evident when comparing the wind direction distributions (measured and those based on the atlases), analyses by Sengers (2019) indicates significant (and anomalous compared to that observed at other measurement locations) mean absolute errors in the wind direction data measured at K13a (20.4º) and EPL (18.6º). Therefore, this should be considered when examining the wind direction results presented below.

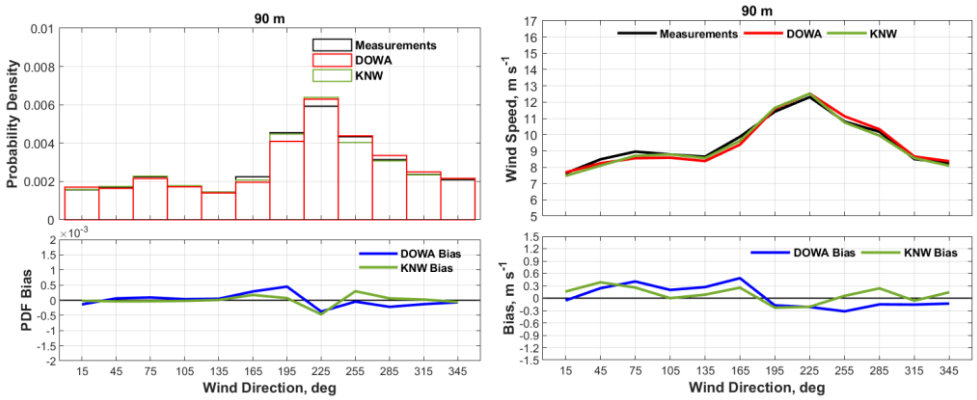

Figure 55 (Left column) Wind direction distribution and the wind direction distribution PDF bias (i.e. $WS_{meas} - WS_{atlas}$) at MMIJ. (Right column) Mean wind speed per wind direction bin and the corresponding bias.

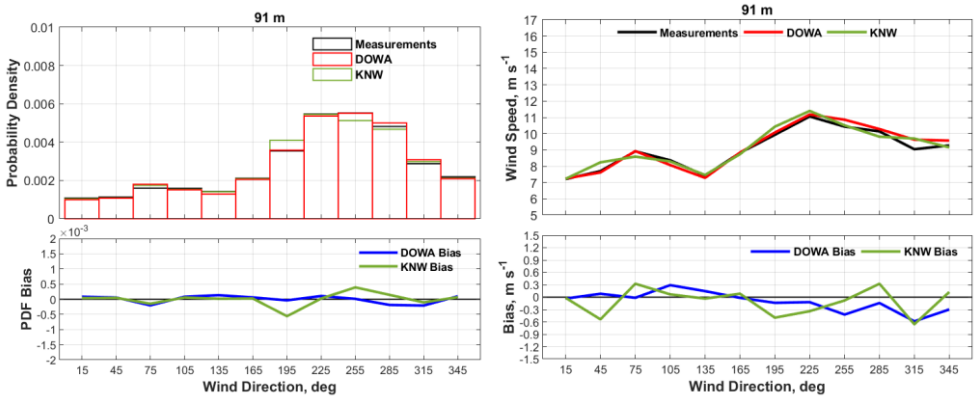

Figure 56 Same as Figure 55 except at K13a.

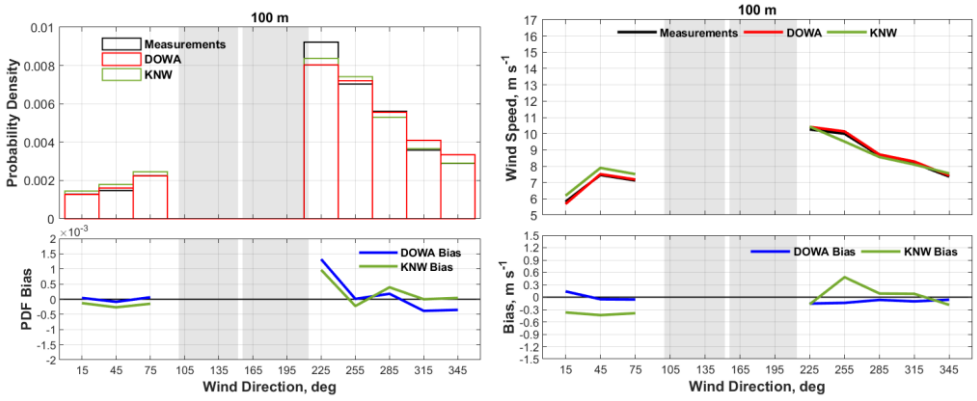

Figure 57 Same as Figure 55 except at HKNa. Shaded areas represent those wind direction sectors filtered to remove wind farm wake effect.

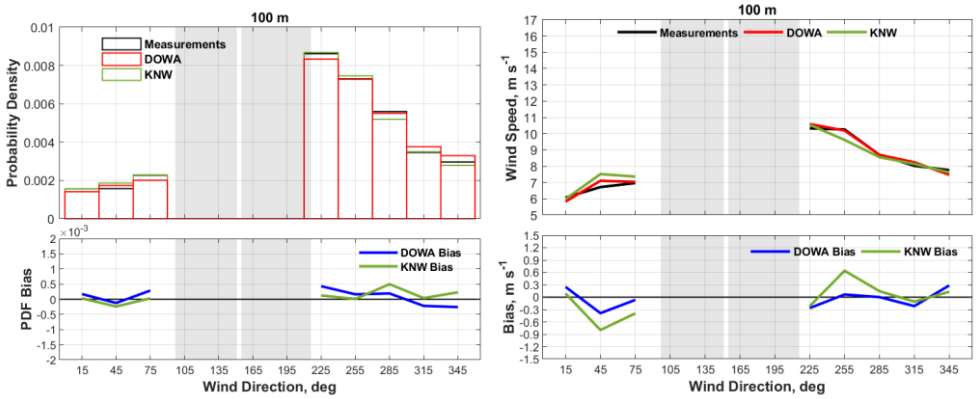

Figure 58 Same as Figure 55 except at HKNb. Shaded areas represent those wind direction sectors filtered to remove wind farm wake effect.

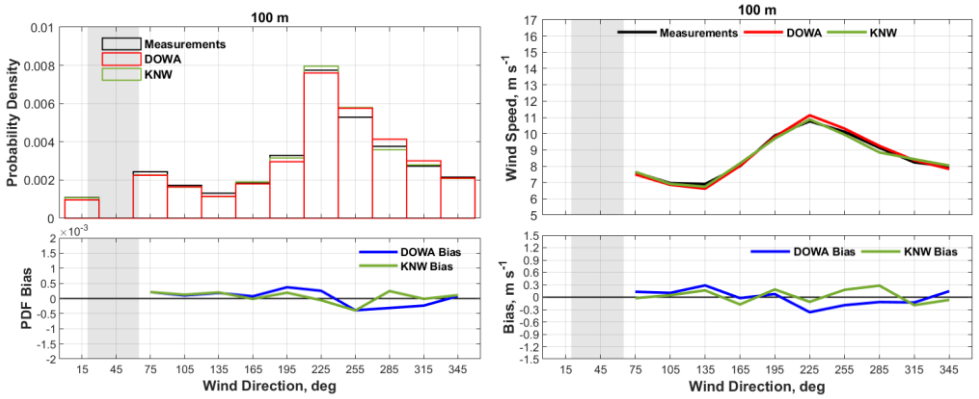

Figure 59 Same as Figure 55 except at HKZa. Shaded areas represent those wind direction sectors filtered to remove wind farm wake effect.

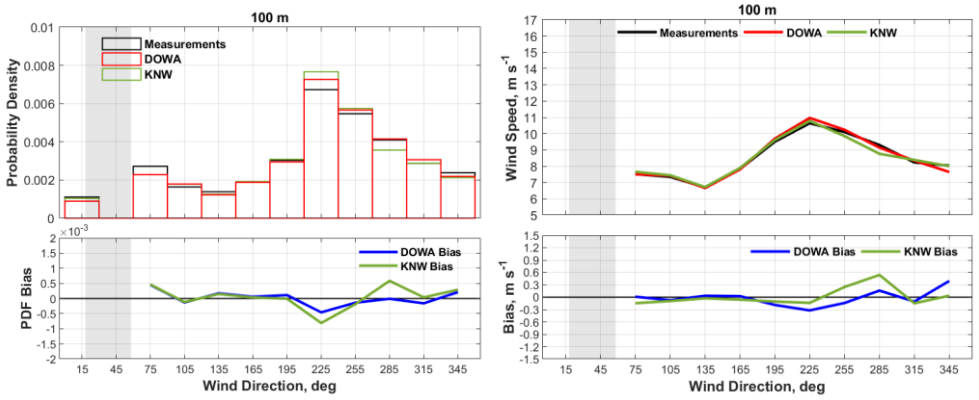

Figure 60 Same as Figure 55 except at HKZb. Shaded areas represent those wind direction sectors filtered to remove wind farm wake effect.

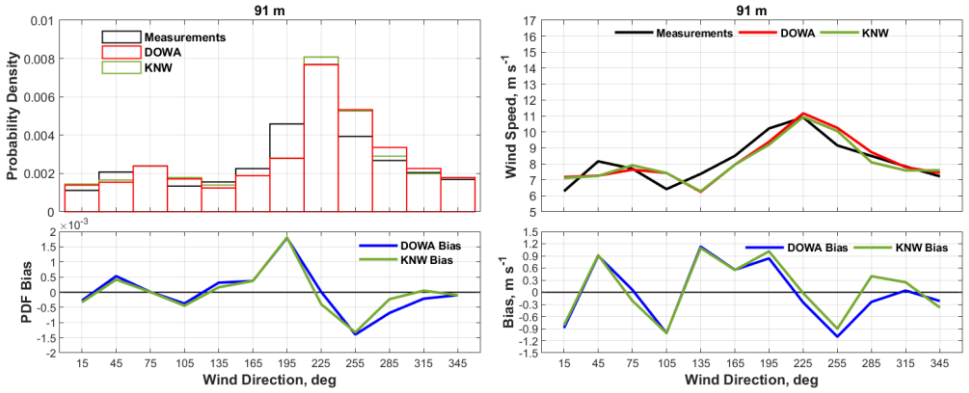

Figure 61 Same as Figure 55 except at EPL.

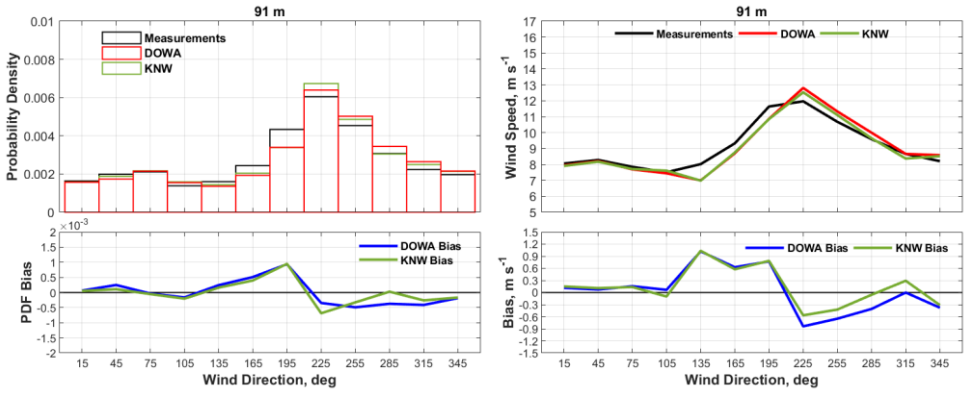

Figure 62 Same as Figure 55 except at LEG.

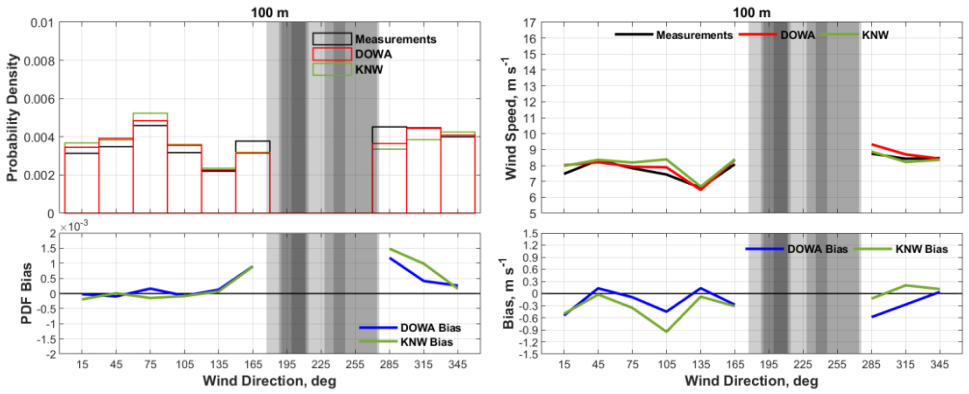

Figure 63 Same as Figure 55 except at BWFZ1. Shaded areas represent those wind direction sectors filtered to remove wind farm wake effect.

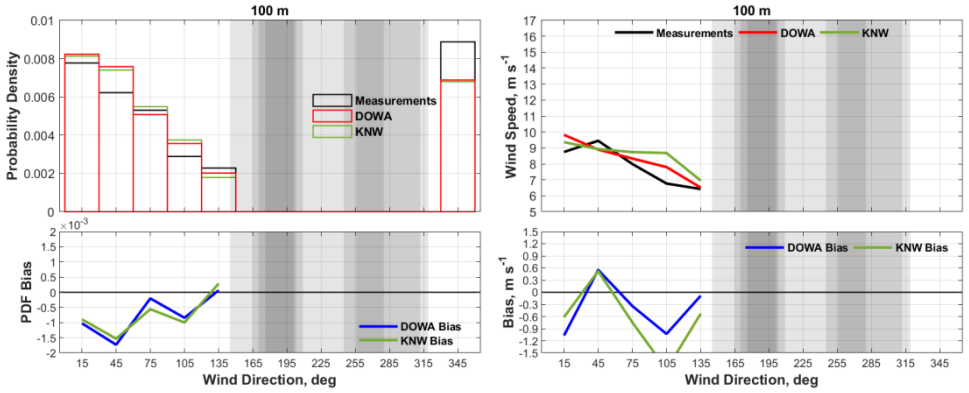

Figure 64 Same as Figure 55 except at Site II. Shaded areas represent those wind direction sectors filtered to remove wind farm wake effect.

4.1.2 Validation of the DOWA against offshore meteorological masts

Wind atlas wind direction distributions were also compared to instrumented meteorological tower measurements at MMIJ (Figure 65) and OWEZ (Figure 66). Similar to the insight gained from comparing wind atlas wind directions to LiDAR measurements, both the KNW-atlas and the DOWA were able to reliably discern the wind direction distribution at MMIJ and OWEZ. Considering all mast measurement heights at MMIJ, the absolute maximum wind direction PDF bias was negative within both the DOWA and the KNW-atlas. At OWEZ, the absolute maximum wind direction PDF bias was positive within both the DOWA and the KNW-atlas. However, the significant wind direction filtering that was imposed at OWEZ due to the location of neighbouring wind farms may have impacted the sign of the absolute maximum bias observed.

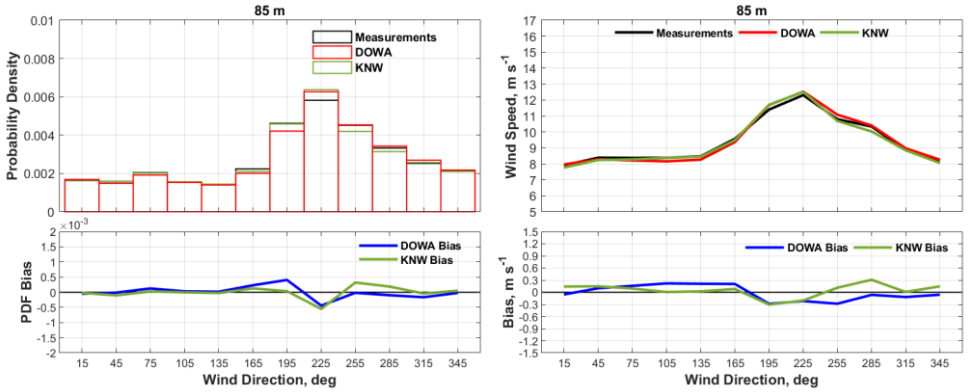

Figure 65 (Left column) Wind direction distribution and the wind direction distribution PDF bias (i.e. $WS_{meas} - WS_{atlas}$) at MMIJ. (Right column) Mean wind speed per wind direction bin and the corresponding bias.

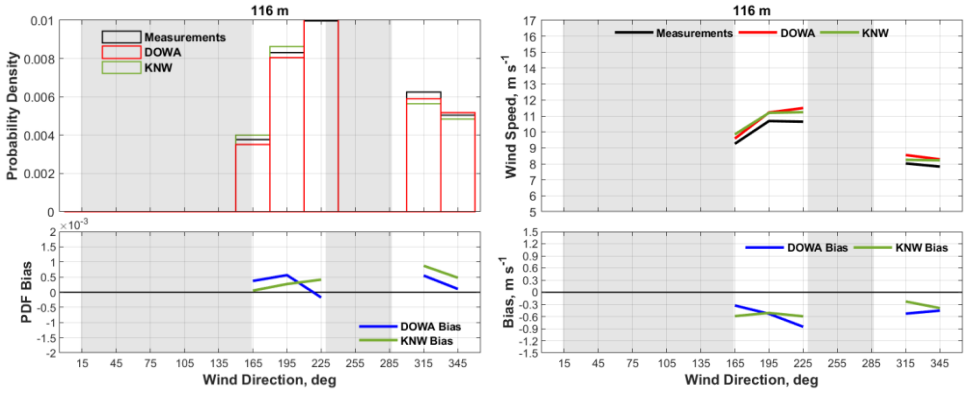

Figure 66 Same as Figure 65 except at OWEZ. Shaded areas represent those wind direction sectors filtered to remove wind farm wake effect.

5 Conclusions

Within the past decade, the KNMI produced the KNW-atlas and the DOWA to depict offshore wind conditions across North Sea. The KNW-atlas was previously validated against instrumented meteorological tower measurements both onshore and offshore and against both QuickSCAT and ASCAT satellite winds (Stepek et al. 2015; Wijnant et al. 2015). The KNW-atlas exhibited a climatological wind speed accuracy of less than 0.2 m/sat all mast locations and measurement heights examined and is able to capture the interannual variability of the North Sea wind climate as it encompasses more than 40 years. However, in order to achieve this accuracy, a uniform shear-correction factor was applied within the KNW-atlas. A limitation of the KNW-atlas is that it exhibits poor hourly correlation, and therefore it is unable to properly represent the diurnal cycle in wind speed. Through the use of new models and methods, the DOWA was developed with the principal objective of improving the hourly wind speed correlation. For wind resource assessments in wind energy applications the correlation with local measurements is the preferred option to reduce the uncertainties for the wind farm business case. As an added bonus, vertical wind shear could be replicated within the DOWA without having to apply the uniform shear-correction factor.

The creation of the DOWA was part of a joint project with ECN part of TNO, Whiffle, and KNMI. The DOWA is a wind atlas based on a global reanalysis dataset (ERA5) that captures 10 years (2008-2017) of meteorological measurements and generates 3D wind fields consistent with these measurements and the laws of physics. This dataset is downscaled using the weather forecasting model HARMONIE with a horizontal grid of 2.5 km. In order to develop the DOWA, an improved version of ECMWFs global reanalysis was used (ERA5) as well as a new version of HARMONIE with improved turbulence parameterizations. Also, the method that was used to make the atlas was improved (i.e. no cold starts and additional assimilation of innovative measurements [e.g. ASCAT and MODE-S EHS]). In this validation report, the performance of the DOWA and the KNW-atlas was validated against wind measurements (wind speed and direction) made by both LiDAR and instrumented meteorological towers. The main conclusions are: (1) the DOWA provides a dataset of wind speed and direction for the North Sea up to 600m height with high quality and large certainty. The differences of the DOWA with measurements at offshore meteorological masts and LiDARs has the same order of magnitude as the measurement uncertainty of the masts and LiDARs, (2) the DOWA improves hourly wind speed correlation compared to KNW, and hence the representation of the diurnal cycle in wind speed, and (3) the DOWA is able to adequately represent vertical wind shear without the incorporation of a uniform shear-correction factor, which was needed in the KNW-atlas to exhibit similar performance. A summary of specific results is provided in the subsection below.

5.1 Summary of results

Validation efforts confirm to what was previously found by Stepek et al. (2015) for validation of the KNW-atlas. Conclusions from these analyses, which were derived from comparison to LiDAR data at eight location and instrumented meteorological tower data at two locations, are provided below.

- The DOWA significantly improved the hourly wind speed correlation with measurements.
  - At each LiDAR measurement location and height, the values of both the linear least-squares regression slope and R^2 indicate improved hourly wind speed correlation within the DOWA. The mean slope value was 0.97 within the DOWA and 0.94 within the KNW-atlas, while the mean R^2 value was 0.91 within the DOWA and 0.87 within the KNW-atlas. Further, these statistics did not significantly degrade with height within the DOWA.
  - Linear least-squares regression between the DOWA and instrumented meteorological tower measurements at MMIJ produced a slope and R^2 value, respectively, of 0.99 and 0.93 at 27m, 0.99 and 0.94 at 58m, and 0.99 and 0.94 at 85m. Alternatively, linear least-squares regression between the KNW-atlas and instrumented meteorological tower measurements at MMIJ produced a slope and R^2 value, respectively, of 0.98 and 0.91 at 27m, 0.97 and 0.91 at 58m, and 0.97 and 0.91 at 85m.
- The representation of seasonal wind speeds between the DOWA and the KNW-atlas was similar.
  - The calendar-month mean wind speed bias at the LiDAR measurement height nearest 100m at all LiDAR measurement locations was -0.062m/s (a slight overestimation) for the DOWA and 0.025m/s (a slight underestimation) for the KNW-atlas.
  - The wind atlas performed well within any specific season.

  Results indicate that the DOWA provides a better representation of the diurnal cycle than KNW.
  - At each LiDAR measurement location and wind atlas forecast hour (i.e. 00,00 UTC, 01:00 UTC, etc.), the DOWA reduced the σ value of the hourly wind speed bias at the LiDAR measurement height nearest 100m compared to KNW
  - On average, the σ value of the hourly wind speed bias was reduced by 0.26m/s (16.99%) from a mean σ value of 1.53m/s within the KNW-atlas to a mean σ value of 1.27m/s within the DOWA.
  - Relative to instrumented meteorological tower measurements at MMIJ, the mean σ value of the hourly wind speed bias across all hourly forecast intervals was 1.10m/s at 27m, 1.18m/s at 58m, and 1.24m/s at 85m within the DOWA, and was 1.31m/s at 27m, 1.40m/s at 58m, and 1.46m/s at 85m within the KNW-atlas. At OWEZ, the DOWA on average reduced the σ value of the hourly wind speed bias by 0.18m/s at 21m, 0.19m/s at 70m, and 0.22m/s at 116m.
- Both wind atlases show good correlation with measurements of the derived Weibull scale (A) and shape (k) parameters with height. Interpret the summary points provided below with the understanding that the DOWA, unlike the KNW-atlas, does not incorporate a uniform shear-correction factor.

- At the LiDAR measurement height nearest 100m, the DOWA exhibited a mean *A* bias of -0.071m/s (overestimation) and the KNW-atlas exhibited a mean *A* bias of only 0.0073m/s (underestimation). Near 200m, both the DOWA and the KNW-atlas overestimated the value of *A*; the DOWA exhibited a mean *A* bias of -0.089m/s and the KNW-atlas exhibited a mean *A* bias of -0.084m/s. Furthermore, at the MLMH, the mean *A* bias was -0.080m/s within the DOWA.

- At the LiDAR measurement location nearest 100m, the KNW-atlas exhibited a mean *k* bias of 0.0025 (underestimation) and the DOWA exhibited a mean *k* bias of 0.023 (underestimation). Similarly, at the LiDAR measurement height nearest 200m, the wind atlases continue to slightly underestimate *k*. The KNW-atlas underestimated *k* by a mean value of 0.0040, while the DOWA underestimated the value of *k* by a mean value of 0.091. At the MLMH, the DOWA underestimate the value of *k* by a mean value of 0.038.

- Relative to instrumented meteorological tower measurements, the DOWA performed significantly better than the KNW-atlas at discerning *k* at lower measurement heights. The *k* bias at MMIJ at 27m was 0.076 for the KNW-atlas and 0.027 for the DOWA. Similarly, the *k* bias at OWEZ at 21m was -0.10 for the KNW-atlas and -0.0052 for the DOWA.

- All of the differences found between the DOWA or the KNW-wind speed profiles and the measurements are within measurement accuracy except at OWEZ.

- The DOWA slightly overestimates mean monthly and annual average wind speeds, while the KNW-atlas slightly underestimates these values.

  - Considering all LiDAR measurement locations and comparable measurement heights (i.e. 90m $\leq$ h $\leq$ 200m), the μ value of the wind speed bias between the wind atlas and LiDAR mean monthly wind speeds was -0.070m/s (overestimation) for the DOWA and 0.019m/s for the KNW-atlas (overestimation).

  - Relative to instrumented meteorological tower measurements at MMIJ, the DOWA overestimated the monthly mean wind speeds by 0.13m/s at 27m, 0.11m/s at 58m, and 0.099m/s at 85m, while the KNW-atlas exhibited a mean monthly wind speed bias of -0.015m/s at 27m, -0.0061m/s at 70m, and 0.0061m/s at 85m.

  - The μ value of the annual wind speed bias between the LiDAR and wind atlas wind speeds at the lidar measurement height nearest 100m was -0.085m/s (overestimation) in the DOWA and -0.015m/s (overestimation) in the KNW-atlas.

  - OWEZ is the only measurement location examined where the KNW-atlas overestimated the monthly mean and annual average wind speeds. The measurements at OWEZ have a relatively large uncertainty as compared to the measurements at meteorological mast IJmuiden or the LiDAR measurements. In addition the measurement mast is closest to shore.

Resolving the land-sea transition is still issue of R&D within the wind energy and meteorological communities.

- The data in both wind atlases show accurate wind direction distributions. On average the wind direction distribution bias to measurements was smaller within the DOWA than within the KNW-atlas.

6 Acknowledgements

The authors would also like to thank Henk van den Brink and Bert van Ulft for their support in the validation of the DOWA. The authors would also like to acknowledge that this project was supported with Topsector Energy subsidy from the Ministry of Economic Affairs and Climate Policy.

7 References

Albers, A. et al., 2013: Ground-based remote sensor uncertainty – a case study for a wind lidar, EWEA 2013

Baas, P., 2014: Final report of WP1 of the WTI2017-HB Wind Modelling project. Scientific Report, WR 2014-02, De Bilt: KNMI.

Banakh, V.A, I. N. Smalikho, F. Köpp, and C. Werner, 1993: Representativeness of wind measurements with CW Doppler LiDAR in the atmospheric boundary layer. *Applied Optics*, **34**, 2055-2067.

Bischoff, O., J. Gottschall, B. Gribben, J. Hughes, D. Stein, J.P. Verhoef and I. Würth, 2016: Offshore Wind Accelerator Recommended Practices for Floating LiDAR Systems, Issue 1.0, 2016.

Brand, A.J., and T. Hegberg, 2004: Wind resource in the Dutch part of the North Sea, ECN-RX—04-132. Presented at the European Wind Energy Conference 2004, London.

Burton, T., N. Jenkins, D. Sharpe, and E. Bossanyi, 2011: Wind energy handbook. John Wiley & Sons, Ltd. Chichester, UK.

Carbon Trust, 2013: Carbon Trust Offshore Wind Accelerator roadmap for the commercial acceptance of floating LIDAR technology, CTC819 Version 1.0, November 2013.

Christiansen, M.B., and C.B. Hasager, 2005: Wake effects of large offshore wind farms identified from satellite SAR. *Remote Sensing of Environment*, **98**, 251-268.

Crockford, A., H. Pater, and E. Holtslag, 2015: Borssele Offshore Wind Farm Zone Wind Resource Assessment, Ecofys report.

De Rooy, W.C., and H. de Vries, 2017: Harmonie verification and evaluation. HIRLAM Technical Report (V70), 79 pp.

Dhirenda, D., A. Crockford and E. Holtslag, 2016: Uncertainty Assessment Fugro OCEANOR SEAWATCH Wind Lidar Buoy at RWE Meteomast Ijmuiden. Ecofys (https://offshorewind.rvo.nl/file/download/45051422)

Donkers, J.A.J., A.J. Brand, and P.J. Eecen, 2011: Offshore Wind Atlas of the Dutch Part of the North Sea, ECN-M—11-031. Presented at the European Wind Energy Association conference 2011, Brussels.

Duncan, J.B., P.A. van der Werff, and E.T.G. Bot, 2018: Understanding of the offshore wind resource up to high altitudes (≤315 m). TNO Technical Report (TNO 2018 R11592).

Eecen, P.J., L.A.H. Machielse and A.P.W.M. Curvers, 2007: Meteorological Measurements OWEZ – Half year report 01-07-2005 – 31-12-2005, ECN-E—07-073.

Geertsema, G.T., and H.W. van den Brink, 2014: Windkaart van Nederland op 100 m hoogte. KNMI Technical Report (TR-351).

Genc, A., M. Erisoglu, A. Pekgor, G. Oturanc, A. Hepbasli, and K. Ulgen, 2005: Estimation of wind power potential using Weibull distribution. *Energy Sources*, **9**, 809-822.

Hersbach, H., 2011: Sea surface roughness and drag coefficients as functions of neutral wind speed. *Journal of Physical Oceanography*, **41**, 247-251.

IEC 2005, IEC 61400-12-1 Wind turbines – Part 12-1: Power performance measurements of electricity producing wind turbines, first edition 2005-12.

IEC 2018, IEC 61400-12-1 Wind energy generating systems – Part 12-1: Power performance measurements of electricity producing wind turbines, Edition 2.0 2017-03.

Kouwenhoven H.J., 2007: User manual data files meteorological mast Noordzee Wind R03, http://www.noordzeewind.nl/wp-content/uploads/2012/02/NZW-16-S-4-R03-Manual-data-files-meteo-mast-NoordzeeWind.pdf

Kudryavstev, V.N., and V.K. Makin, 2007: Aerodynamic roughness of the sea surface at high winds. *Boundary-layer meteorology*, **125**, 289-303.

Maureira Poveda, J.P. and D.A.J. Wouters, 2015: Wind Measurements at Meteorological Mast Ijmuiden. ECN-E--14-058

Medley, J., 2014: Classification of ZephIR 300 LiDAR at the UK remote sensor test site, ZephIR Lidar https://www.zxlidars.com/wp-content/uploads/2014/12/ZephIR-300-Classification-Report.pdf.

METEK, 2013: Ultrasonic Wind Sensor uSonic-3 Scientific previously USA-1, Metek-Ultrasonic-Anemometer-uSonic-3-Scientific-USA-1-Datasheet.pdf

Pedersen, T.F., and Coauthors, 2006: ACCUWIND – Accurate wind speed measurements in wind energy. DTU Summary Report (Risø-r-1563).

Peña, A., C.B. Hasager, S.-E. Gryning, M. Courtney, I. Antoniou, and T. Mikkelsen, 2009: Offshore wind profiling using light detection and ranging measurements. *Wind Energy*, **12**, 105-124.

Rehman, S., A.M. Mahbub Alam, J.P. Meyer, and L.M. Al-Hadhrami, 2012: Wind speed characteristics and resource assessment using Weibull parameters. *International Journal of Green Energy*, **9**, 800-814.

Seity, Y., P. Brousseau, S. Malardel, G. Hello, P. Bénard, F. Bouttier, C. Lac, and V Masson, 2011: The AROME-France convective-scale operational model. *Monthly Weather Review*¸**139**, 976-991.

Sengers, B.A.M., 2019: On the potential of data assimilation of turbine wind measurements in HARMONIE. KNMI Internship Report.

Stepek, A., M. Savenije, H.W. van den Brink, and I.L. Wijnant, 2015: Validation of KNW-atlas with publicly available mast observations (Phase 3 of KNW project). KNMI Technical Report (TR-352).

Toros, H., G. Geertsema, G. Cats, 2014: Evaluation of the Hirlam and Harmonie Numerical Weather Prediction Models during air pollution episode over Greater Istanbul Area. CLEAR – Soil, Air, Water, **42**, 863-870.

van den Brink, H.W., I.L. Wijnant, F.C. Bosveld, and A. Stepek, 2017: Klimatologie van extreme windvlagen. KNMI Wetenschappelijk rapport (WS 20147-01).

Wagenaar, J.W., D.A.J Wouters and J.P. verhoef, 2015: Ring analysis floating LiDAR, static LiDAR and offshore meteorological mast. Conference proceedings EWEA 2015. ECN-M--15-047

Werkhoven, E.J. and J.P. Verhoef, 2012: Offshore meteorological Mast Ijmuiden. Abstract of Instrumentation Report. ECN-Wind Memo 12-010

Westermann, D., 2019: Summary report VT121244 – Version 1.0 3D Sonic Anemometer Classification, Summary_Thies_3D_Sonic_final_Version1.pdf.

Wieringa, J., and P.J. Rijkoord, 1983: Windklimaat van Nederland. Staatsuitgeverij Den Haag.

Wijnant, I.L., H.W. van den Brink, and A. Stepek, 2014: North Sea wind climatology part 2: ERA-Interim and Harmonie model data. KNMI Technical Report (TR-343).

Wijnant, I.L., G.J. Marseille, A. Stoffelen, H.W. van den Brink, and A. Stepek, 2015: Validation of the KNW-atlas with scatterometer winds (Phase 3 of the KNW project). KNMI Technical Report (TR-353)

Wouters, D.A.J. and J.P. Verhoef, 2019: Verification of Leosphere Windcube WLS7-577 at ECN part of TNO LiDAR Calibration Facility, for offshore measurements at Lichteiland Goeree. TNO 2019 R10398

Wouters, D.A.J. and J.P. Verhoef, 2019: Verification of ZephIR 300 unit 315 at ECN part of TNO LiDAR Calibration Facility, for offshore measurements at Euro Platform (EPL). TNO 2018 R10762

Wouters, D.A.J. and J.P. Verhoef, 2019: Verification of ZephIR 300 unit 563 at ECN part of TNO LiDAR Calibration Facility, for offshore measurements at K13-A production platform. TNO 2018 R10850

A Determination of wind speed and direction from boom arm measurements

A.1 Methods at MMIJ

ECN part of TNO applied the following algorithm at MMIJ to determine the 'true' wind speed and direction that was used for validation of the wind atlases at MMIJ. However, prior to defining the algorithm, the following variables are established.

$\overline{WD}$	Mean wind direction measured across all three boom arms
$\overline{WD}_{NE}$	Mean 10-min wind direction measured along the 46.5º boom arm
$\overline{WD}_{SSE}$	Mean 10-min wind direction measured along the 166.5º boom arm
$\overline{WD}_{WNW}$	Mean 10-min wind direction measured along the 286.5º boom arm
$\overline{TD}$	True wind direction (**used in the validation efforts**)
$\overline{WS}_{NE}$	Mean 10-min wind speed measured along the 46.5º boom arm
$\overline{WS}_{SSE}$	Mean 10-min wind speed measured along the 166.5º boom arm
$\overline{WS}_{WNW}$	Mean 10-min wind speed measured along the 286.5º boom arm
$\overline{TS}$	True wind speed (**used in the validation efforts**)

Algorithm that was used to determine $\overline{TD}$:

If $(\overline{WD} > 16.5^0$ and $\overline{WD} \leq 76.5^0)$ or $(\overline{WD} > 196.5^0$ and $\overline{WD} \leq 256.5^0)$, then

$$\overline{TD} = \frac{1}{2}(\overline{WD}_{SSE} + \overline{WD}_{WNW})$$

Else

If $(\overline{WD} > 76.5^0$ and $\overline{WD} \leq 136.5^0)$ or $(\overline{WD} > 256.5^0$and $\overline{WD} \leq 316.5^0)$, then

$$\overline{TD} = \frac{1}{2}(\overline{WD}_{NE} + \overline{WD}_{SSE})$$

Else

$$\overline{TD} = \frac{1}{2}(\overline{WD}_{NE} + \overline{WD}_{WNW})$$

Endif

Algorithm that was used to determine $\overline{TS}$:

If $(\overline{TD} > 46.5^0$ and $\overline{TD} \leq 166.5^0)$ then

$$\overline{TS} = \frac{1}{2}(\overline{WS}_{NE} + \overline{WS}_{SSE})$$

Else

If $(\overline{TD} > 166.5^0$ and $\overline{TD} < 286.5^0)$ then

$$\overline{TS} = \frac{1}{2}(\overline{WS}_{SSE} + \overline{WS}_{WNW})$$

Else

$$\overline{TS} = \frac{1}{2}(\overline{WS}_{NE} + \overline{WS}_{WNW})$$

Endif

Further clarification of these methods can be found in Werkhoven and Verhoef (2012).

A.2 Methods at OWEZ

At OWEZ, averaging of measurements made along different boom arms was not performed. Instead, measurements that were made along the boom arm that was 'least disturbed' by the tower structure were for validation of the wind atlases. The following conditions were used to determine the relevant boom arm measurements.

- For wind directions between 0º and 120º, measurements made along the 60º (NE) boom arm were used.
- For wind directions between 120º and 240º, measurements made along the 180º (S) boom arm were used.
- For wind directions between 240º and 360º, measurements made along the 300º (NW) boom arm were used.

This method is in accordance with those previously used to validate the KNW-atlas (Stepek et al. 2015).

B Data quality control

Data quality control is imperative to ensure the validity of the DOWA validation efforts performed herein. Implementation of data quality control varied depending upon both the measurement source (i.e. LiDAR versus mast) and LiDAR type (i.e. ZephIR 300s versus WINDCUBE v2). However, an effort was made to ensure the quality assurance measures employed were relatively uniform between the measurement sites. The LiDARs at the BWFZ, HKN, and HKZ measurement locations were also subject to first-order quality control that was performed by Fugro; an overview of these quality control procedures can be found online at https://offshorewind.rvo.nl. The other quality control measures performed by ECN part of TNO are detailed below.

B.1 Plausible value checks

Regardless of the measurement source (i.e. LiDAR or mast), plausible value checks were imposed on the wind data. Any 10-min value that satisfied the following criteria were removed from the data record and were not used for the DOWA validation.

- The mean wind speed was either greater than the period maximum wind speed or less than the period minimum wind speed.
- The mean wind speed was less than 0.05m/s.
- Turbulence intensity (TI) for the period fell below 0.10% (i.e. 0.001).
- At the measurement height, the value of TI was 10 standard deviations (σ_{TI}) greater than the mean (μ_{TI}) TI value (i.e. $TI \geq \mu_{TI} + 10\sigma_{TI}$); μ_{TI} and σ_{TI} were defined as the height-respective value for the entire data collection period. Because TI typically decreases with mean wind speed, this threshold was only imposed if the 10-min mean wind speed exceeded 4 m/s.

B.2 LiDAR-specific quality control

Quality control measures specific to the LiDAR data were also applied. Any 10-min observation that satisfied the following criteria were removed from the data record and similarly were not used in during the validation of the DOWA.

- A LiDAR error code (e.g. 9998 or 9999) was reported.
- A carrier-to-noise ratio (CNR) (i.e. a measure of signal quality) less than -22. CNR information was only outputted with the WINDCUBEv2 LiDAR data.
- Backscatter magnitude less than $1e^{-5}$ or greater than 100. Backscatter served as a proxy for CNR for the ZephIR 300s wind LiDAR data wherein CNR information was not available.
- Data availability within the 10-min period less than 80%.

Note that the LiDAR data provided by Fugro did not contain the signals required to implement the backscatter and data availability requirements. Therefore, these two quality control measures were not be employed. However, this does not mean that Fugro did not independently apply similar quality control measures.

The ZephIR 300s wind LiDAR uses a compact met station equipped with a sonic anemometer to determine the sign of the wind direction. The use of this sonic anemometer can sometimes lead to a 180º wind direction error (Peña et al. 2009), especially at low wind speeds. Analysis performed by ECN part of TNO of LiDAR wind data at MMIJ collected across a two-year period indicated that this flow-reversal error was evident in approximately 3.6% of the data record (Poveda and Wouters 2014). This flow-reversal can be identified and mitigated by comparing the LiDAR wind directions to an independent wind direction source—typically a meteorological mast. However, at each of the measurement locations used in the validation of DOWA, an independent measurement source was not always available. Therefore, instead of using collocated mast measurements to mitigate this error, wind direction data from the DOWA was used. If the absolute difference between the DOWA and LiDAR wind directions was between 160º and 200º (i.e. $\pm$20º from 180º), then the LiDAR wind direction was not considered in the validation of the DOWA. However, because wind directions can vary significantly at lower wind speeds, this difference was only examined when the LiDAR wind speed was greater than 4m/s. These 180º wind direction errors do not impact the quality of the measured wind speeds.

B.3 Filtering to remove wind farm wake effects

The DOWA produces an undisturbed wind climatology that excludes any potential atmospheric effects that may be caused by neighbouring wind farms. Therefore, in order to prevent wind farm wakes from adversely impacting the DOWA validation efforts, data from certain wind direction sectors were filtered. Prior research using synthetic-aperture radar (SAR) indicates that within unstable and near-neutral atmospheric conditions, the wind farm wake can extend outwards of 20km downstream (Christiansen and Hasager 2005). Although the wind farm wake is expected to grow with increasing atmospheric stability, a 20km length was used to denote the maximum wake impact distance of a neighbouring wind farm. Therefore, for each measurement location, it was determined whether there was a neighbouring wind farm within 20 km. If a neighbouring wind farm was detected, wind data from those wind directions impacted by the wind farm were not considered in the validation of the DOWA. Wind measurements (wind speed and direction) emanating from the identified wind direction sectors were ignored in analyses beginning on the date of wind farm construction (per the Global Offshore Wind Farm Database [https://www.4coffshore.com/windfarms/]).

C Vertical profiles of wind speed

C.1 Validation of the DOWA against offshore LiDAR

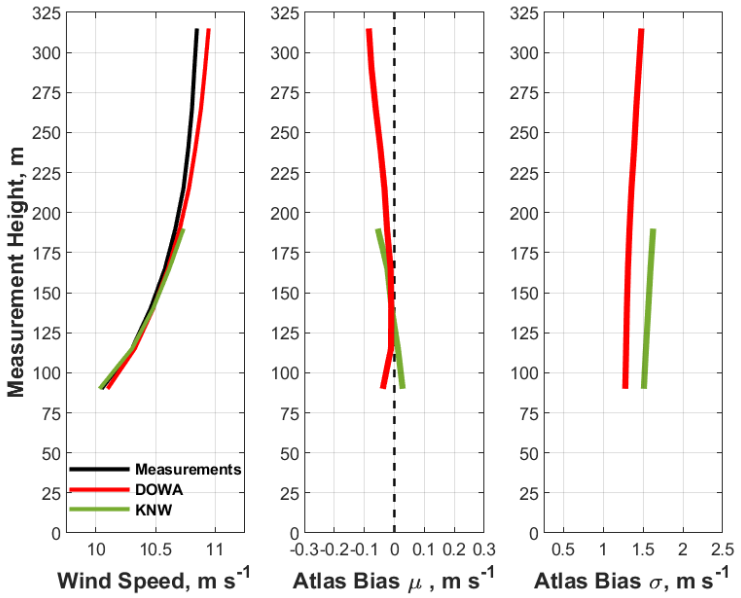

Figure C.1 (Left column) Vertical profile of wind speed as defined by LiDAR, the KNW-atlas, and the DOWA at MMIJ. The (middle column) μ and (left column) σ values of the DOWA wind speed bias (i.e. $WS_{meas} - WS_{atlas}$).

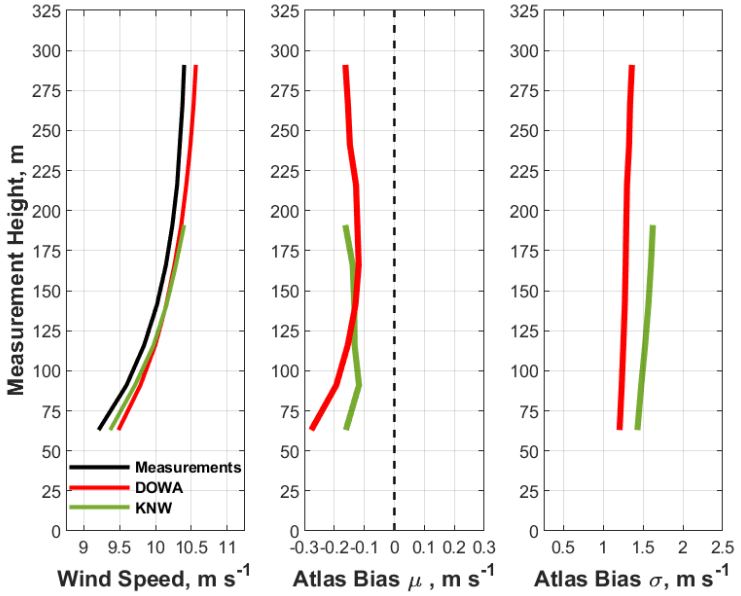

Figure C.2 Same as Figure C.1 except at K13a.

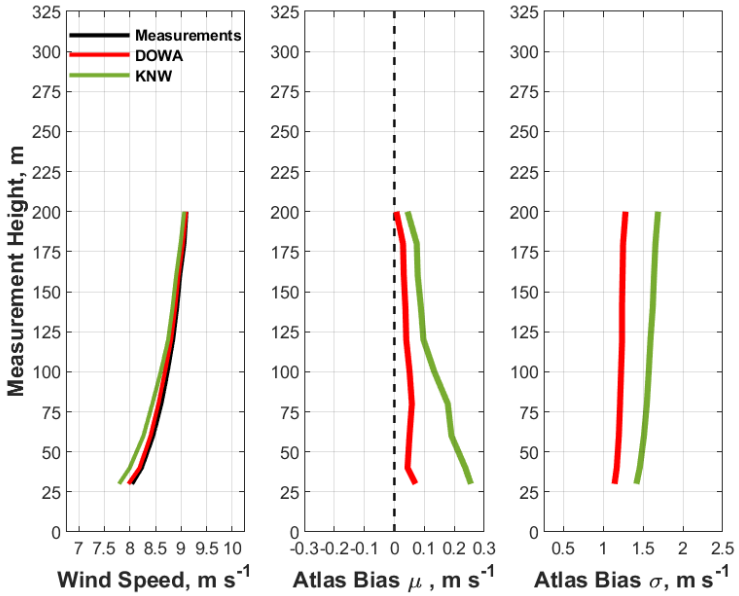

Figure C.3 Same as Figure C.1 except at HKNa.

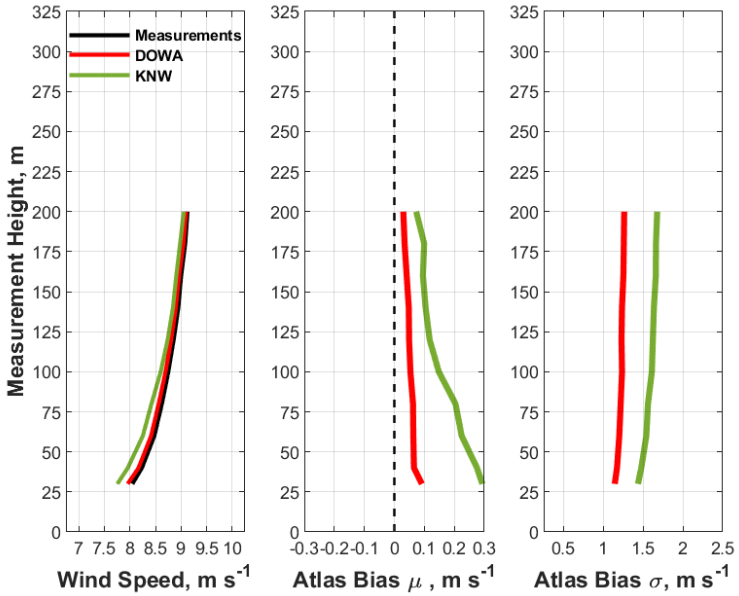

Figure C.4 Same as Figure C.1 except at HKNb.

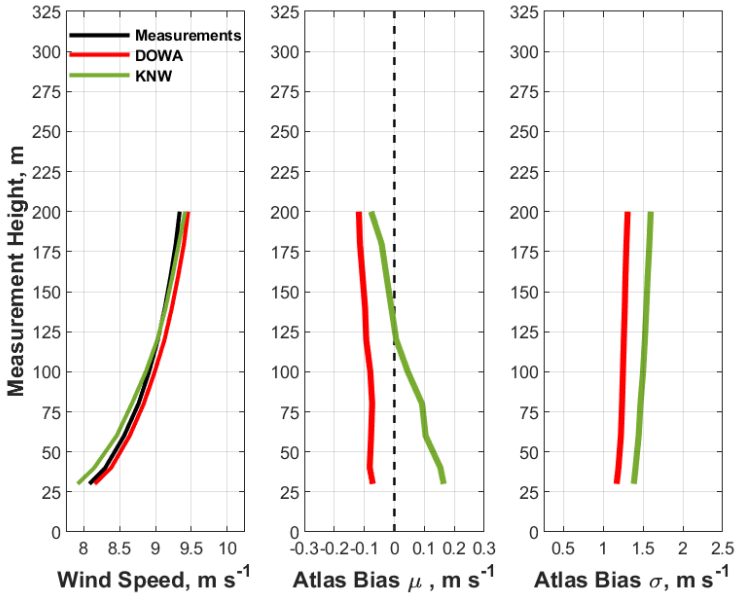

Figure C.5 Same as Figure C.1 except at HKZa.

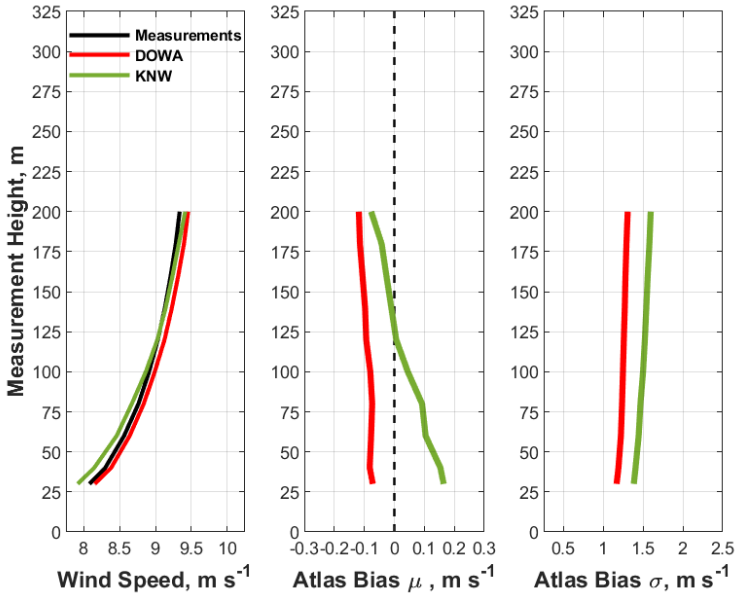

Figure C.6 Same as Figure C.1 except at HKZb.

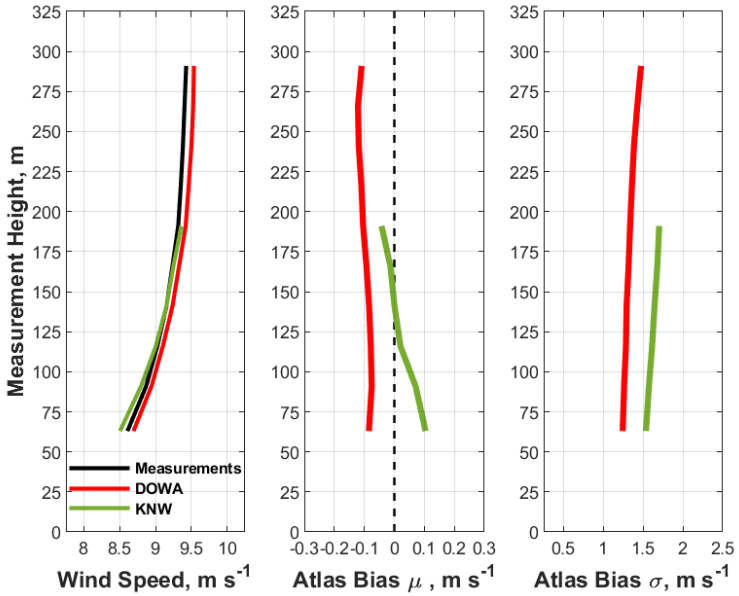

Figure C.7 Same as Figure C.1 except at EPL.

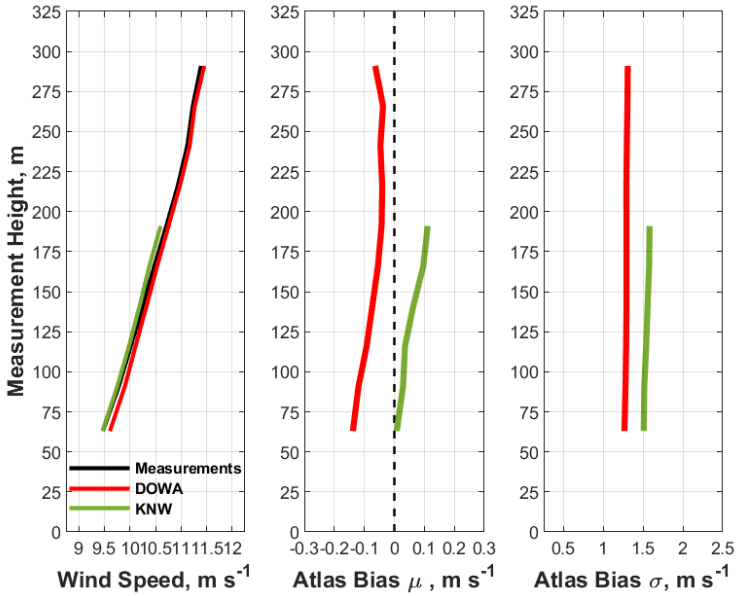

Figure C.8 Same as Figure C.1 except at LEG.

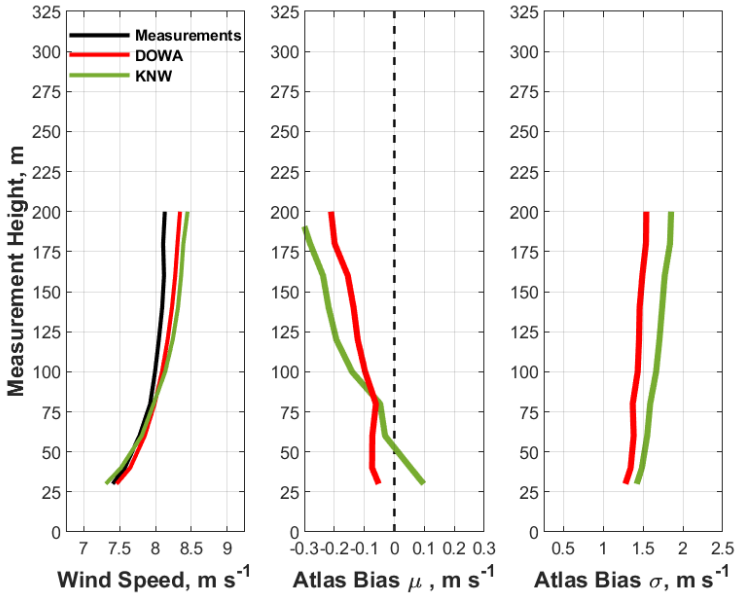

Figure C.9 Same as Figure C.1 except at BWFZ1.

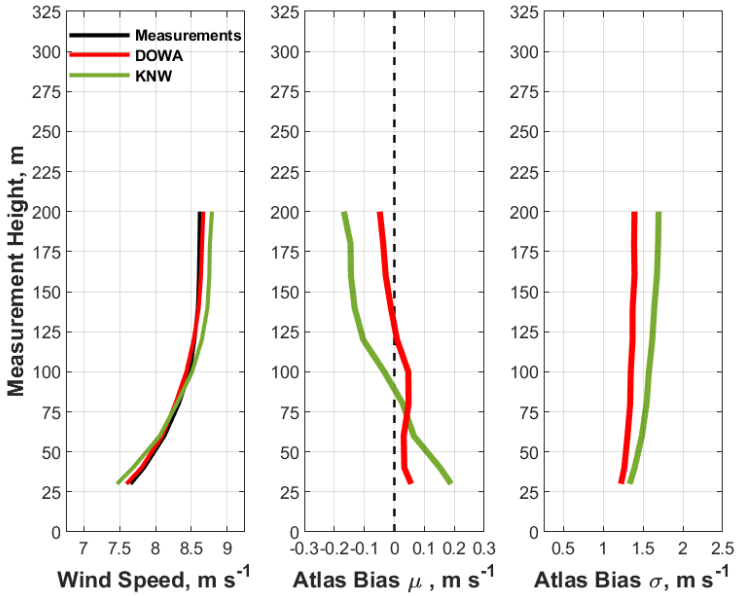

Figure C.10 Same as Figure C.1 except at BWFZ2.

C.2 Validation of the DOWA against offshore meteorological masts

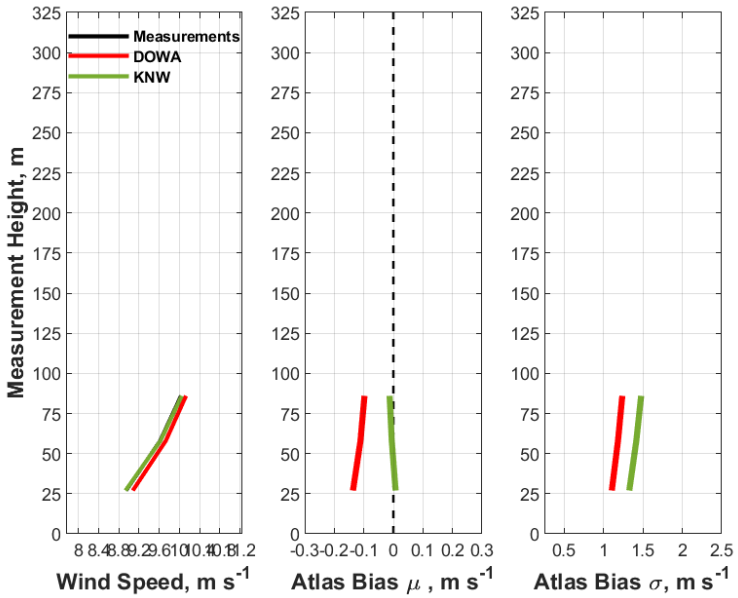

Figure C.11 (Left column) Vertical profile of wind speed as defined by the instrumented meteorological mast, the KNW-atlas, and the DOWA at MMIJ. The mean (middle column) μ and (left column) σ values of the DOWA wind speed bias (i.e. $WS_{meas} - WS_{atlas}$).

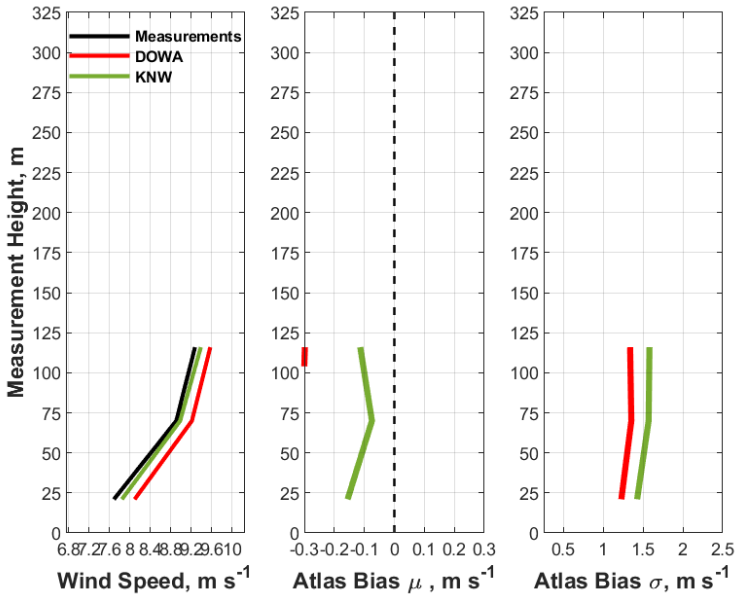

Figure C.12 Same as Figure C.11 except at OWEZ. Except at 116m, the μ DOWA bias at OWEZ is outside the plotted range of values (i.e. $\mu_{DOWA} \leq -0.3$ m/s).